

UCSF

UC San Francisco Electronic Theses and Dissertations

Title

Identifying a Role for the ER Stress Sensor IRE1 α in Fatty Acid-Induced Inflammation

Permalink

<https://escholarship.org/uc/item/6xh6s2t1>

Author

Robblee, Megan

Publication Date

2016

Peer reviewed|Thesis/dissertation

Identifying a Role for the ER Stress Sensor IRE1 α in Fatty
Acid-Induced Inflammation

by

Megan M. Robblee

DISSERTATION

Submitted in partial satisfaction of the requirements for the degree of

DOCTOR OF PHILOSOPHY

in

Biomedical Sciences

in the

GRADUATE DIVISION

of the

UNIVERSITY OF CALIFORNIA, SAN FRANCISCO

Copyright 2016
by
Megan M. Robblee

ACKNOWLEDGEMENTS

I am immensely thankful for the support of my family, friends, and colleagues, without whom my graduate school experience would have been considerably less fruitful and enjoyable. My parents, Dick and Nancy, have always valued education and urged me to pursue my interests, academic or otherwise, with dedication and enthusiasm. They raised me to be the scientist I am today, and I am grateful for their ever-present support and encouragement. Growing up, my older sister Betsy was my model of scholastic achievement and set a high bar for me to meet or exceed in my own schooling. Now that we are adults, she still leads the way in inspiring me to follow my passion, and I couldn't ask for a better companion for camping trips and food safaris.

My friends and classmates in the BMS program have served as critical sounding boards and an understanding support network through the challenges and stresses of grad school. I have fond memories of pizza talks, costume parties, Tahoe hijinks, and TMR practices during our early days and tamer reunion barbeques in our more mature years. I particularly thank my fellow metabolism devotee, Jillian, and my past and present roommates Allyson, Joan, and Bianca, who have provided advice, space, distraction, and entertainment as needed, and friendship always.

Over the course of my PhD, I have spent more time with my lab-mates than anyone else. I am therefore fortunate to have shared this experience with such quality people, who have guided me through my struggles, taught me how to be a better scientist, and provided much-needed levity. Thank you to Martin, the model of productivity and reliability; Diana, for clinical insight and sympathetic chats; Jess, my lab buddy and mother hen; Annie, for her kindness and generosity; and the many volunteers, rotation students, and visiting scholars who have enriched the lab with their spirit and enthusiasm. I'm also appreciative of Allison Xu, Christian Vaisse, and their respective labs for insightful discussion and constructive criticism during joint lab

meetings and journal clubs, and my thesis committee, Scott Oakes, Averil Ma, and Ari Molofsky, for their helpful advice and feedback.

Lastly, this dissertation would not have been possible without the direction and encouragement of my mentor, Suneil Koliwad. I couldn't have asked for a more positive, accessible, and supportive PI who has enabled me to both develop as a scientist and enjoy the process all along the way. Suneil's energy and optimism sets the tone for the lab, and I have always felt valued and respected thanks to his leadership.

CONTRIBUTIONS TO THE PRESENTED WORK

The Materials and Methods, Results, and Discussion sections of this dissertation are a reprint of the material as it appears in *Cell Reports* under the citation below. This published work was primarily conducted and written by Megan M. Robblee while enrolled at UCSF and is comparable in scope and contribution to a standard dissertation. – *Suneil K. Koliwad, M.D., Ph.D., Mentor*

Megan M. Robblee, Charles C. Kim, Jess Porter Abate, Martin Valdearcos, Karin L.M. Sandlund, Meera K. Shenoy, Romain Volmer, Takao Iwawaki, Suneil K. Koliwad (2016). Saturated fatty acids engage an IRE1 α -dependent pathway to activate the NLRP3 inflammasome in myeloid cells. *Cell Reports* 14, 2611-23.

M.M.R. and S.K.K. conceived of and designed the research. M.M.R. performed the majority of the experiments, with contributions from M.V. (immunoblotting and immunofluorescence), K.L.M.S. (SVF analysis), and R.V. (expression of mutant IRE1 α). J.P.A. conducted the microarray and performed preliminary analyses, along with M.S. and M.M.R. C.C.K. performed final bioinformatic analyses of the array data and created the resulting figures. T.I. provided the ERAI-Luciferase mice. M.M.R. analyzed all of the data, with guidance from S.K.K., and drafted the manuscript with feedback from M.V. and J.P.A. M.M.R. then wrote the final manuscript with advice and editorial supervision from S.K.K.

Thank you to Dr. Joachim Schultze and his laboratory for making available their human macrophage array data and the laboratory of David Ron, University of Cambridge, for reagents and advice. Technical assistance was provided by Hui Wang, the Gladstone Institutes Genomics

and Bioinformatics Cores, the UCSF Cytometry and Cell Sorting Core and Biological Imaging Development Center, and the UCSF Diabetes Center Metabolic Phenotyping Core and Microscopy Core. This work was supported by NIH grants 5K08DK080174 (to S.K.K.), P30DK063720 (UCSF DRC), and P30DK098722 (UCSF NORC), and a NSF Graduate Research Fellowship (to M.M.R.).

Identifying a Role for the ER Stress Sensor IRE1 α in Fatty Acid-Induced Inflammation

Megan M. Robblee

ABSTRACT

Diets rich in saturated fatty acids (SFAs) produce a form of tissue inflammation driven by “metabolically activated” macrophages, which contributes to the development of obesity-associated metabolic diseases. To better understand this form of macrophage activation, we analyzed the transcriptomes of mouse macrophages treated with either SFAs or the classical inflammatory stimulus lipopolysaccharide (LPS). SFA treatment induced a transcriptional signature distinct from that of LPS and strongly enriched by endoplasmic reticulum (ER) stress markers. In particular, SFA treatment increased the expression of the ER stress sensor IRE1 α and many of its target genes comprising the adaptive unfolded protein response. SFAs also activate the NLRP3 inflammasome in macrophages, resulting in secretion of the pro-inflammatory cytokine IL-1 β . We found that IRE1 α mediates SFA-induced IL-1 β secretion by macrophages and that its activation by SFAs does not rely on unfolded protein sensing. Instead, the ability of SFAs to stimulate either IRE1 α activation or IL-1 β secretion can be specifically reduced by preventing their flux into the phosphatidylcholine (PC) class of membrane lipids or by increasing unsaturated PC levels. Thus, IRE1 α is an unrecognized intracellular PC sensor critical to the process by which SFAs stimulate macrophages to secrete IL-1 β , a driver of diet-induced tissue inflammation and metabolic dysfunction.

TABLE OF CONTENTS

INTRODUCTION	1
<i>The global problem of metabolic disease and the unmet need for therapies</i>	1
<i>The role of metabolic inflammation in the pathogenesis of obesity-associated disease</i>	2
<i>Saturated fatty acids (SFAs) as triggers of metabolic inflammation</i>	3
<i>The NLRP3 inflammasome and other inflammatory pathways activated by SFAs</i>	6
<i>Links between SFAs, the ER stress sensor IRE1α, and inflammation</i>	7
<i>Mechanisms of IRE1α activation by SFAs</i>	10
<i>Summary and open questions</i>	11
MATERIALS AND METHODS	13
RESULTS	22
<i>SFA treatment produces a transcriptional signature distinct from LPS treatment and defined by the induction of genes associated with the ER and UPR</i>	22
<i>SFA treatment preferentially induces adaptive, but not terminal, IRE1α signaling in both mouse and human macrophages</i>	26
<i>IRE1α is progressively and reversibly activated in mice consuming excess saturated fat</i>	30
<i>SFAs act intracellularly to activate IRE1α and the NLRP3 inflammasome</i>	32
<i>IRE1α endoribonuclease activity is required for SFA-induced NLRP3 inflammasome activation</i>	35
<i>SFAs and classical UPR activators induce Xbp1 splicing by distinct mechanisms</i>	39
<i>Intracellular SFAs flux in a manner that is distinct from UFAs and not controlled by UFA levels</i>	44
<i>The flux of SFAs into phosphatidylcholine contributes to IRE1α and NLRP3 inflammasome activation</i>	48
<i>Summary</i>	52
DISCUSSION	54
REFERENCES	60

LIST OF TABLES

Table 1: Primers used for quantitative RT-PCR

18

LIST OF FIGURES

Figure 1. SFA and LPS treatments induce distinct patterns of gene expression in BMDMs	23
Figure S1 (Related to Figure 1). SFAs and LPS induce inflammatory activation through distinct mechanisms	25
Figure 2. SFA treatment preferentially induces adaptive, but not terminal, IRE1 α signaling in both mouse and human macrophages	28
Figure S2 (Related to Figure 2). SFAs do not induce widespread RIDD activation or cell death in BMDCs.	29
Figure 3. IRE1 α is progressively and reversibly activated in mice consuming excess saturated fat	31
Figure 4. Long-chain SFAs activate IRE1 α and the NLRP3 inflammasome through an intracellular mechanism	33
Figure S3 (Related to Figure 4). Responses to SFAs and LPS in BMDMs and BMDCs	34
Figure 5. IRE1 α endoribonuclease activity is required for SFA-induced NLRP3 inflammasome activation	36
Figure S4 (Related to Figure 5). SFA-induced NLRP3 inflammasome activation does not involve TXNIP induction or ROS	38
Figure 6. Co-treatment with UFAs specifically mitigates SFA-induced IRE1 α and NLRP3 inflammasome activation	40
Figure S5 (Related to Figure 6). Combination of PBA and OA does not diminish SFA-induced IRE1 α or NLRP3 inflammasome activation more than PBA or OA alone	41
Figure S6 (Related to Figure 6). SA treatment robustly activates IRE1 α and PERK but not ATF6 α	43
Figure S7 (Related to Figure 6). OA and PA flux to distinct lipid compartments, and OA co-treatment does not modulate the pattern of PA flux	45
Figure S8 (Related to Figure 6). DGAT1 activity does not control SFA-induced IRE1 α or NLRP3 inflammasome activation	47
Figure S9 (Related to Figure 7). Limiting the flux of SFAs into sphingolipids does not reduce SFA-induced IRE1 α or NLRP3 inflammasome activation	48
Figure 7. Limiting the ability of SFA treatment to increase phospholipid saturation blocks consequent IRE1 α and NLRP3 inflammasome activation	51

Figure 8: Model depicting activation of IRE1 α and the NLRP3 inflammasome by SFAs in macrophages.

53

INTRODUCTION

The global problem of metabolic disease and the unmet need for therapies

Economic development and improvements in the world's food supply have reduced the frequency of famine and mortality from under-nutrition, but they have also shifted activity and dietary patterns in a way that poses new challenges to public health. Greater availability and consumption of inexpensive processed foods and animal products rich in sugar and saturated fat, coupled with increasingly sedentary lifestyles, have led to a global rise in obesity and chronic diseases stemming from over-nutrition in both developed and lower-income countries (Chopra et al., 2002). The World Health Organization estimates that non-communicable diseases such as diabetes, heart disease, stroke, and hypertension (components of the metabolic syndrome) will supplant infectious diseases as the principle cause of global morbidity and mortality by 2020 (World Health Organization, 1997). As such, obesity and its co-morbidities present an enormous and growing public health challenge and economic burden that necessitates public policy, educational, and medical interventions.

Despite the global obesity epidemic, therapeutic strategies to combat obesity and metabolic diseases are inadequate. Lifestyle modifications to alter diet, exercise, and behavior patterns have limited efficacy in producing dramatic and long-lasting weight reduction (Wadden et al., 2012). Though modest weight loss can improve some markers of metabolic health and prevent the progression of diabetes (Knowler et al., 2002), even intensive lifestyle interventions are unable ameliorate other components of the metabolic syndrome, such as cardiovascular morbidity and mortality in overweight and obese patients with type 2 diabetes (Look AHEAD Research Group et al., 2013). Pharmacological interventions are therefore in demand, and

research aimed at better understanding the deleterious effects of the so-called “Western diet” is urgently needed to identify ways to curtail the rise in obesity and metabolic disease.

The role of metabolic inflammation in the pathogenesis of obesity-associated disease

Prolonged consumption of a diet high in saturated fat leads to a chronic inflammatory response that contributes to metabolic dysregulation and disease. This state, termed “metabolic inflammation”, involves changes in the number, composition, and activation profile of innate and adaptive immune cells in metabolic tissues such as adipose tissue, muscle, liver, pancreas, and the brain. Of these, myeloid cells (MCs) such as adipose tissue macrophages (ATMs) play a key role in inciting and perpetuating the inflammatory response. In lean individuals, resident ATMs function to maintain homeostasis through tissue remodeling and secretion of anti-inflammatory and immunoregulatory cytokines. High fat diets promote recruitment of MCs and other immune cell subsets to adipose, liver, and muscle (Nguyen et al., 2007; Stefanovic-Racic et al., 2012; Weisberg et al., 2003), where they initiate and/or perpetuate an inflammatory milieu by secreting pro-inflammatory cytokines and promoting the infiltration and activation of additional immune cells (Lumeng et al., 2007).

The resulting local and systemic inflammation is considered a driving factor in the pathogenesis of a number of metabolic diseases, including type 2 diabetes and atherosclerosis. In rodent models, ablating MCs (Patsouris et al., 2008) or disrupting the function of key pro-inflammatory signaling pathways and cytokines globally (Cai et al., 2005; Hirosumi et al., 2002; Yuan et al., 2001) or specifically in MCs (Arkan et al., 2005; Solinas et al., 2007) alleviates diet-induced insulin resistance and many other adverse metabolic consequences of the Western diet.

However, the therapeutic utility of this approach is limited by the added risk of infections when innate immunity is broadly impaired.

A critical barrier is therefore the lack of understanding of specific mechanisms by which the Western diet induces inflammation and metabolic dysfunction that can be targeted without causing generalized immunosuppression or other adverse effects. This first requires identifying what it is about the Western diet that provokes inflammation and what distinguishes metabolic inflammation from immune responses against pathogens.

The MCs found in obese adipose tissue share markers with “classically activated” macrophages responding to bacterial lipopolysaccharide (LPS) or other molecular signals indicative of bacterial or viral infection (pathogen-associated molecular patterns; PAMPs) or tissue damage (danger-associated molecular patterns; DAMPs). These features include activation of NF κ B and JNK signaling pathways and secretion of pro-inflammatory cytokines such as TNF, IL-6, and IL-1 β . Thus, ATMs were often described as having an “M1” polarization in obesity (Lumeng et al., 2007). More recent studies have revealed that obesity results in a distinct polarization state in ATMs defined by lipid metabolism programs rather than classical inflammatory pathways (Kratz et al., 2014; Xu et al., 2013). Probing the nature of this “metabolically activated” (M_{Me}) macrophage signature could reveal pathways that mediate inflammation in response to obesity-associated triggers but not infectious stimuli.

Saturated fatty acids (SFAs) as triggers of metabolic inflammation

What initiates this inflammatory response in obesity? Two main hypotheses have emerged. In the first, changes in gut microbiome composition and intestinal barrier function with obesity allow microbial products (e.g. LPS and other PAMPs) to enter the circulation and

activate the innate immune system via pattern recognition receptors (PRRs) such as toll-like receptors (TLRs). The second hypothesis proposes that pro-inflammatory dietary components and endogenous signals released from stressed tissues recruit and activate MCs and other immune cells. These models, detailed below, are not mutually exclusive, and exogenous and endogenous triggers could synergistically promote tissue inflammation.

Though the chronic, low-level inflammatory response observed with adipose tissue hypertrophy is often described as a form of sterile inflammation, elevated circulating levels of the endotoxin LPS and other PAMPs are observed in obese humans and rodents (Cani et al., 2007; Kallio et al., 2015). These microbial products activate PRRs to stimulate cytokine production and systemic inflammation (Cani et al., 2007). The mechanism for this metabolic endotoxemia is incompletely understood, but it likely involves changes in the composition of the gut microbiota. Obesity is associated with a shift in the abundance of microbial classes that favors increased energy harvest from the diet (Turnbaugh et al., 2006). Indeed, transplantation of gut microbes from obese mice into lean mice is sufficient to transmit the obese phenotype (Turnbaugh et al., 2006). These changes in microbiome composition may also impair gut barrier function and allow microbial endotoxins to enter the circulation, as increased intestinal permeability and disrupted tight junctions have been observed in some rodent obesity models (Brun et al., 2007; Cani et al., 2008).

Another hypothesis is that the saturated fatty acids (SFAs) that predominate in the Western diet are themselves pro-inflammatory and impair the metabolic functions of tissues when in excess. The deleterious effects of ectopic lipid accumulation were first appreciated in pancreatic beta cells (Y. Lee et al., 1994), but this concept of lipotoxicity extends to a variety of cell types, including immune cells. Saturated fatty acids (SFAs) in particular trigger

inflammatory signaling and cellular dysfunction when in excess, whereas unsaturated fatty acids (UFAs) do not cause lipotoxicity and can mitigate many of the effects of SFAs (L'homme et al., 2013; Welters et al., 2004).

MCs in metabolic tissues such as adipose are routinely exposed to fluctuating levels of SFAs released by neighboring adipocytes or circulating lipoproteins based on the nutritional state of the animal. Adipocytes store fatty acids in the form of triacylglycerol (TG) within their lipid droplets. During periods of fasting, lowered insulin levels promote the breakdown of this TG by lipolysis to liberate fatty acids for energy. This process is dysregulated in obesity when adipocytes become resistant to the action of insulin to repress lipolysis in the fed state, resulting in increased release of fatty acids from adipocytes. In addition to being bathed in SFAs derived from adipocyte lipolysis, ATMs are also confronted with abrupt lipid loads upon phagocytosis of cellular debris, particularly from dying adipocytes. Treatment of MCs in vitro with SFAs to mimic this physiological lipid exposure is sufficient to reproduce the transcriptional signature of metabolically activated macrophages isolated from the adipose tissue of obese mice (Kratz et al., 2014). Stressed and dying adipocytes also release other signals such as adipokines, cytokines, and DAMPs that may stimulate the infiltration and activation of MCs and other immune cells.

The lipotoxicity response of MCs to SFAs encompasses activation of classical M1 inflammatory signaling pathways involving NF κ B and JNK and secretion of pro-inflammatory cytokines such as IL-6 and TNF (J. Y. Lee et al., 2001), activation of the NLRP3 inflammasome, and production of IL-1 β and IL-18 (Reynolds et al., 2012; Wen et al., 2011), induction of the unfolded protein response (UPR) and markers of endoplasmic reticulum (ER) stress, and ultimately apoptosis. Each of these outcomes is evident in the MC-containing stromal-vascular fraction (SVF) of adipose tissue from obese mice and humans (H. Li et al., 2010; Lumeng et al.,

2007; Sharma et al., 2008; Weisberg et al., 2003) and has been linked to metabolic disease in animal models (Arkan et al., 2005; Erbay et al., 2009; Maris et al., 2012; Ozcan et al., 2006; Solinas et al., 2007; Tsukano et al., 2010; Wen et al., 2011). These findings lend credence to the idea that dietary SFAs are mediators of metabolic inflammation, but how they exert their toxic effects remains an open question.

The NLRP3 inflammasome and other inflammatory pathways activated by SFAs

In the search for key pathways in MCs that mediate the lipotoxic responses to SFAs and diets enriched in them, much attention has been focused on TLR4, a receptor for bacterial LPS that was initially thought to bind dietary SFAs. Though direct binding of SFAs to TLR4 has not been demonstrated (Schaeffler et al., 2009), an adaptor protein, Fetuin A, has been proposed to mediate this interaction (Pal et al., 2012). The classical (M1) inflammatory response to SFAs in MCs is largely dependent on TLR4 signaling (Shi et al., 2006), but TLR4 activation alone does not reproduce other components of MC lipotoxicity, such as NLRP3 inflammasome activation, ER stress, and apoptosis. Mice in which the MCs and other hematopoietic cells are deficient in TLR4 are largely protected from tissue inflammation induced by a high fat diet (Orr et al., 2012; Saberi et al., 2009), but corresponding improvements in glucose metabolism have not been consistently observed (Coenen et al., 2009; Orr et al., 2012; Saberi et al., 2009). This suggests that other lipotoxicity outcomes such as UPR activation and apoptosis that are maintained in TLR4-deficient MCs (Anderson et al., 2012) could contribute to metabolic dysfunction. Additional evidence that SFAs do not merely exert their pro-inflammatory effects at the cell surface through TLR4 comes from many studies in which pharmacologic and genetic

perturbations of intracellular lipid metabolism modulate SFA-induced inflammatory activation of MCs (Galic et al., 2011; Håversen et al., 2009; Koliwad et al., 2010).

In addition to stimulating TLR4-dependent classical inflammatory pathways, SFAs also activate the NLRP3 inflammasome (Reynolds et al., 2012; Wen et al., 2011), an intracellular protein complex that processes the pro-inflammatory cytokines IL-1 β and IL-18 in response to recognition of select PAMPS and DAMPS. Circulating IL-1 β levels are elevated in obesity and thought to contribute to metabolic dysfunction by promoting tissue inflammation, impairing insulin signaling, and triggering death of pancreatic beta cells (Jager et al., 2007; Wen et al., 2011). Deletion or antagonism of IL-1 β , its receptor, or components of the NLRP3 inflammasome ameliorates markers of tissue inflammation and insulin resistance in mouse models of diet-induced obesity (de Roos et al., 2009; Osborn et al., 2008; Stienstra et al., 2010; Vandanmagsar et al., 2011; Wen et al., 2011).

Activation of the NLRP3 inflammasome is a two-step process. A first “priming” signal is required to induce transcription of pro-IL-1 β and pro-IL-18 and components of the inflammasome, which can be mediated by ligation of toll-like receptors (TLRs) or cytokine receptors that activate NF κ B signaling. A second signal then induces assembly of these components, NLRP3, ASC, and pro-caspase-1, which results in activation of caspase-1 to cleave pro-IL-1 β and pro-IL-18 to their mature forms for secretion. SFAs can provide this second signal to induce IL-1 β secretion in MCs primed with LPS (Wen et al., 2011). Mechanisms proposed for this effect involve ceramide production (Schilling et al., 2012) and increased production of ROS due to impairment of AMPK-regulated autophagy (Wen et al., 2011).

Links between SFAs, the ER stress sensor IRE1 α , and inflammation

An alternative pathway that could mediate NLRP3 inflammasome activation by SFAs centers on inositol-requiring enzyme 1-alpha (IRE1 α), one of three transducers of endoplasmic reticulum (ER) stress that induce the unfolded protein response (UPR). ER stress occurs in response to an imbalance between the capacity of the ER to facilitate protein folding and maturation and its cargo load of nascent proteins destined for secretion or residence in the endomembrane system, resulting in an accumulation of unfolded or misfolded proteins in the ER. This can occur due to a variety of physiological conditions, such as oxidative stress, hypoxia, depletion of calcium from the ER, nutrient depletion or excess, high cargo load, or exposure to pathogens or pharmacological agents. The ER stress sensors IRE1 α , PERK, and ATF6 recognize the accumulation unfolded proteins and initiate the UPR to restore ER homeostasis. This “adaptive UPR” involves inhibition of translation to reduce the protein-folding demand, production of additional chaperones to facilitate folding, and upregulation of the ER-associated degradation (ERAD) system to target misfolded proteins for export from the ER and degradation by the proteasome. If the stress cannot be rectified, the “terminal UPR” is engaged to direct the cell toward apoptosis.

IRE1 α is an integral membrane protein of the ER consisting of a luminal domain that senses ER stress and cytoplasmic domains with kinase and endoribonuclease activities responsible for its signaling functions. The luminal domain of IRE1 α mediates its activation when unfolded proteins accumulate in the ER lumen and either directly bind to IRE1 α and/or cause the dissociation of the chaperone BiP from the luminal domain (Bertolotti et al., 2000; Credle et al., 2005). IRE1 α then oligomerizes and *trans*-autophosphorylates, leading to activation of its endoribonuclease activity and unconventional splicing of the mRNA encoding the transcription factor X-box-binding protein 1 (XBP1) (H. Li et al., 2010). The spliced *Xbp1*

transcript is then translated and regulates the homeostatic transcriptional program of the UPR. During severe or prolonged ER stress, higher-order oligomers of IRE1 α form, and the specificity of the endoribonuclease domain is relaxed such that other ER-localized transcripts are cleaved (Han et al., 2009; Hollien et al., 2009). This process, termed regulated IRE1-dependent decay (RIDD), can relieve the protein-folding burden of ER but is also associated the induction of the terminal UPR and apoptosis.

The UPR, and the IRE1 α arm in particular, is robustly activated by SFAs in cultured MCs and other cells (Anderson et al., 2012). High fat diets also induce ER stress in adipose and liver (Ozcan et al., 2004; D. Wang et al., 2006), which might be mediated in part by excess exposure to SFAs. Dietary manipulations have shown that accumulation of SFAs in the liver is correlated with elevated IRE α activity and other measures of ER stress, whereas mice that accumulate UFAs to a similar extent are protected from ER stress in the liver (D. Wang et al., 2006). These ER stress responses in metabolic tissues are likely to contribute to metabolic dysfunction, as treatment of obese mice with chemical chaperones to reduce ER stress alleviates insulin resistance in liver and peripheral tissues (Ozcan et al., 2006).

While the mechanism for these improvements has not been well established, reduced tissue inflammation could play a role given the intersections between the UPR and key inflammatory signaling nodes. IRE1 α can induce JNK and NF κ B signaling via recruitment of the adaptor TRAF2 to the phosphorylated cytoplasmic domains of IRE1 α (Kaneko et al., 2003; Urano et al., 2000). More recently, IRE1 α activation under conditions of chemically induced ER stress was also shown to activate the NLRP3 inflammasome in THP-1 monocytes primed with LPS (Lerner et al., 2012). Strong chemical inducers of ER stress such as thapsigargin and tunicamycin activate IRE1 α 's RIDD activity, leading to the degradation of miR-17, a microRNA

that negatively regulates translation of thioredoxin-interacting protein (TXNIP) (Lerner et al., 2012). The resulting stabilization of TXNIP activates the NLRP3 inflammasome, resulting in IL-1 β secretion and cell death by pyroptosis (Lerner et al., 2012; Osowski et al., 2012).

However, it is not known whether IRE1 α mediates NLRP3 inflammasome activation by SFAs, and the broader role of IRE1 α in MCs in the context of high fat diet-induced inflammation and insulin resistance has not been investigated.

Mechanisms of IRE1 α activation by SFAs

Though excess SFAs are well known to induce ER stress, the mechanism by which they do so remains incompletely understood. SFA treatment causes depletion of ER calcium stores (Cunha et al., 2008; Wei et al., 2009), which could impair the function of calcium-requiring chaperones such as calreticulin, BiP, and GRP94 and result in accumulation of unfolded proteins that activate of the UPR (Mekahli et al., 2011). This calcium leakage and other impairments of ER function may stem from physical disruption of the ER and loss of its membrane integrity, as dramatic dilation of ER cisternae can be observed upon SFA treatment (Borradaile et al., 2006; Leamy et al., 2014).

Lipid stress can also directly impair ER calcium homeostasis. Whereas non-lipotoxic UFAs are largely incorporated into triacylglycerol (TG) within lipid droplets, an inert storage pool though to sequester fatty acids away from biochemical pathways associated with lipotoxicity (Koliwad et al., 2010; Listenberger et al., 2003), SFAs are poorly stored in TG and instead are incorporated into membrane phospholipids and sphingolipids (Boslem et al., 2011). This alters the composition of ER membranes by increasing the proportion of saturated fatty acyl chains (Ariyama et al., 2010; Borradaile et al., 2006; Ostrander et al., 2001) and shifting the

ratios of specific phospholipid and sphingolipid species such as phosphatidylcholine and phosphatidylethanolamine (Boslem et al., 2011; Fu et al., 2011). Enrichment of ER microsomes with saturated phospholipids or phosphatidylcholine to simulate SFA-induced changes in membrane lipid composition reduces the activity of the ER calcium pump SERCA and thereby limits calcium re-entry into the ER (Fu et al., 2011; Y. Li et al., 2004).

In addition to provoking the UPR by causing unfolded proteins to accumulate, perturbations of cellular lipid homeostasis can also directly activate IRE1 α (Volmer et al., 2013). This was first recognized in yeast, where the IRE1 α ortholog Ire1 is activated by depletion of the membrane lipid component inositol or changes in membrane composition in a mechanism not requiring the luminal domain (Promlek et al., 2011). More recently, the luminal domain was also found to be dispensable for IRE1 α activation by membrane lipid alterations in mammalian cells (Volmer et al., 2013). Increased lipid saturation of reconstituted liposomes was sufficient to activate a truncated form of IRE1 α incapable of sensing unfolded proteins, suggesting that IRE1 α can directly sense the lipid composition of the ER membrane (Volmer et al., 2013). The propensity of IRE1 α to induce *Xbp1* splicing vs. RIDD when activated by this alternative mechanism has not been explored. The PERK arm of the UPR can also be activated by changes in membrane composition (Volmer et al., 2013), and a similar mechanism has been described by which SFAs induce the clustering and activation of the tyrosine kinase c-Src within SFA-enriched membrane domains, leading to downstream JNK activation (Holzer et al., 2011).

Summary and open questions

In the search for key pathways in MCs that mediate the lipotoxic responses to SFAs and diets enriched in them, IRE1 α has emerged as a compelling candidate for several reasons: (1)

IRE1 α is robustly activated by SFAs and obesogenic diets, (2) IRE1 α is linked to the NLRP3 inflammasome and other inflammatory pathways implicated in metabolic disease, and (3) pharmacological interventions to prevent the activation of IRE1 α and other ER stress sensors improve metabolic function in DIO models. However, much remains to be understood about the functional significance of IRE1 α in MCs in obesity and metabolic disease. These questions include how SFAs activate IRE1 α , the role of IRE1 α in SFA-induced NLRP3 inflammasome activation in MCs, and how IRE1 α figures into the broader “metabolic activation” program of MCs treated with SFAs.

Here, we identify that the transcriptional program defining SFA-induced M_{Me} polarization is distinct from that of M_{LPS} polarization and is marked by a prominent ER stress signature, which preferentially includes targets of IRE1 α -dependent *Xbp1* splicing in both mouse and human MCs. We show in mice that excess dietary SFA consumption induces both *Xbp1* splicing and NLRP3 inflammasome activation within the ATM-rich compartment of the white adipose tissue (WAT). Indeed, we demonstrate that IRE1 α is a critical mediator of SFA-induced NLRP3 inflammasome activation in macrophages, and that SFAs activate IRE1 α by increasing the saturation of membrane phospholipids.

MATERIALS AND METHODS

Isolation of primary mouse bone marrow-derived MCs: All procedures were approved by the Institutional Animal Care and Use Committee at the University of California, San Francisco. Wild type, ERAI-Luc (Iwawaki et al., 2009), *Tlr4*^{-/-} (Poltorak et al., 1998), *Dgat1*^{-/-} (Chen et al., 2002a), and aP2-*Dgat1* (Chen et al., 2002b) mice on a C57Bl/6 background and *Cd11b-Cre/Ern1*^{fl/fl} mice (Iwawaki et al., 2009) on a mixed 129/C57Bl/6 background were group-housed and fed a standard chow diet (LabDiet 5053) in a barrier facility with a 12-hour light-dark cycle. Bone marrow cells were isolated from mice euthanized with Avertin and differentiated for 6-8 days in RPMI 1640 (Gibco) containing 10% FBS (Atlanta Biologicals), penicillin/streptomycin, and either recombinant GM-CSF (for bone marrow-derived dendritic cells [BMDCs]) or M-CSF (for bone marrow-derived macrophages [BMDMs]; 10 ng/mL; Peprotech).

Microarray sample preparation: Replicate wells (n = 3-4) of WT BMDMs were treated with LPS (1 ng/mL), stearic acid (SA; 250 μ M), oleic acid (OA; 250 μ M), or bovine serum albumin (BSA; 125 μ M) as a vehicle control for 5 or 20 hours as indicated. Purified DNase-treated total RNA was analyzed for quality using chip-based capillary electrophoresis (Bioanalyzer, Agilent, Inc) and quantity and purity was determined with a NanoDrop spectrometer. The NuGEN Pico V2, based on Ribo-SPIA technology, was used for amplification, fragmentation, and biotin-labeling of ~10 ng input RNA. The labeled cDNA was hybridized to GeneChip Mouse Gene 1.0 ST microarrays (Affymetrix, Santa Clara, CA). Signal intensities of fluorescent images produced during GeneChip hybridizations were read by an Affymetrix Model 3000 Scanner and converted into GeneChip probe results files (CEL) using Command and Expression Console software

(Affymetrix). Array data are available in the NCBI Gene Expression Omnibus (GEO) under the accession number GSE77104.

Microarray data analysis: Data were quantile normalized and median centered across samples as described (Baccarella et al., 2013). Differentially expressed genes were identified using Significance Analysis of Microarrays (Tusher et al., 2001) using two-class unpaired comparisons with 3% false discovery rate (FDR) and 1.5-fold change cutoffs. Clustering was performed with xcluster (Gollub and Sherlock, 2006) and visualized as heatmaps using Java Treeview (Saldanha, 2004). Gene set intersections were determined using custom Perl scripts. Principal component analysis was performed in R. Functional enrichment analysis utilized DAVID (Huang et al., 2009). Human monocyte-derived macrophage datasets were downloaded from GEO (Accession number GSE46903) and processed identically to our mouse datasets. Only data from GM-CSF-derived macrophages treated for 24 hours with 150 μ M SA and corresponding baseline controls were used in our analysis. The intersection of mouse and human genes significantly induced by SA was identified using custom scripts.

In vivo luminescence imaging: Male ERAI-Luc mice (Iwawaki et al., 2009) fed chow or HFD (Harlan Teklad TD.88137) starting at 4-6 weeks of age were imaged in the IVIS Spectrum (PerkinElmer) under isoflurane anesthesia 10 minutes after intraperitoneal injection of luciferin (150 mg/kg, GoldBio). Whole body radiance was quantified using Living Image software (PerkinElmer).

SVF isolation: Visceral adipose tissue (epididymal, perirenal, and mesenteric fat pads) was collected from PBS-perfused 16-24 week old male C57Bl6 mice after consumption of chow or HFD (Harlan Teklad TD.88137) for 12 weeks. Approximately 1 g of pooled VAT was digested for 1 h in a 37 °C shaking incubator with 0.66 mg/mL Type I Collagenase (Worthington) in Krebs Ringer Buffer with 1% BSA, filtered through a 100 µm cell strainer, and centrifuged at 200 x g from 10 minutes to separate the SVF from the adipocytes. SVF pellets were incubated in ACK buffer for 5 minutes to lyse the erythrocytes and resuspended in TRIzol reagent (Life Technologies) for RNA isolation.

Isolation of primary bone marrow-derived MCs: Bone marrow was flushed and pooled from the femurs and tibias of mice (6-12 week old, mixed gender), triturated in RPMI 1640 (Gibco), filtered through a 70 µm cell strainer, and incubated in ACK buffer for 5 minutes. Bone marrow cells were plated in non-tissue culture treated multi-well plates at a density of 2000 cells/mm² and cultured in RPMI supplemented with 10% FBS (Atlanta Biologicals), penicillin/streptomycin, and 10 ng/mL of either recombinant GM-CSF (for BMDCs; Peprotech) or recombinant M-CSF (for BMDMs; Peprotech). Media was replenished on day 3 and replaced on day 6. Growth factors were removed from the media after 6-8 days of differentiation, and adherent cells were used for experiments 1-10 days later.

FA preparation: FAs (Nu-Chek Prep) were dissolved in 70 °C water, and 1 M NaOH was added drop-wise to yield a clear solution (Listenberger et al., 2001). The resulting aqueous FA preparations (20 mM) were complexed at a 2:1 FA:BSA molar ratio with 20% FA-free, low-endotoxin BSA (Sigma Aldrich A8806) heated to 37 °C. FA stock concentrations were measured

using a colorimetric NEFA assay kit (Wako), and aliquots were stored at -20 °C. FA stocks prepared this way had very low levels of endotoxin contamination according to colorimetric LAL assays (Lonza).

Liposome preparation: DOPC liposomes were supplemented with 10% dioleoylphosphatidylserine (DOPS) to both enhance cellular uptake of the liposomes and aid in the formation of small unilamellar vesicles, which do not always form readily from preparations of 100% PC. To accomplish this, chloroform stocks of DOPC and DOPS (Avanti Polar Lipids) were combined at a 10:1 molar ratio of DOPC:DOPS (2 µg total), dried down under a stream of nitrogen, lyophilized for 3 hours, and rehydrated with 1 mL PBS in a 65 °C shaker for 1 hour. Liposome preparations were then sonicated in a 65 °C water bath until they turned clear (2-3 hours) and stored at 4 °C. Prior to addition to media, liposome preparations were heated to 65 °C and sonicated for 10-15 minutes.

FA uptake: BMDCs were pre-treated with 500 µM sulfosuccinimidyl oleate (SSO; Toronto Research Chemicals) in DMSO or DMSO alone for 45 minutes prior to co-treatment with 500 µM PA containing 0.5 µCi/mL ¹⁴C-PA (Moravek Biochemicals) for 4 hours. Media was then removed, and cells were washed three times with Krebs Ringer Buffer containing 0.5% BSA and 500 µM phloretin (Santa Cruz Biotechnology) and lysed with 1 M NaOH. Lysate radioactivity was measured by liquid scintillation counting.

FA flux: BMDCs were treated for 16 hours with 100 µM PA or OA containing 0.1 µCi/mL ¹⁴C-PA or ¹⁴C-OA (Moravek Biochemicals), respectively. Unlabeled OA (20 µM) was added to cells

treated with radiolabeled PA in order to determine the impact of OA co-treatment on intracellular PA flux. After incubation, cells were washed three times with PBS and cellular lipids were extracted using 2:1 chloroform:methanol (Bligh and Dyer, 1959). Lipids in the lower organic phase were dried down under a stream of nitrogen, resuspended in chloroform, spotted on silica plates (Whatman), and resolved by thin layer chromatography using either hexane:ethyl ether:acetic acid (80:20:2) to separate neutral lipids or methyl acetate:isopropanol:chloroform:methanol:0.25% aqueous KCl (25:25:25:10:9) to separate phospholipids (Vitiello and Zanetta, 1978). Air-dried TLC plates were exposed to iodine vapor to visualize bands, and reference standards were used to identify lipid species. Radioactivity was then detected with a Fuji Scanner FLA-5100 phosphorimager and quantified using Multigauge software (Fujifilm).

Real-time quantitative PCR: RNA was isolated using TRIzol reagent (Life Technologies), and 0.2-1 μ g total RNA was reverse-transcribed using the Superscript III Reverse Transcriptase (Life Technologies) and random hexamers according to the manufacturer's instructions. Quantitative RT-PCR was performed on an ABI Prism 7900HT using Power SYBR Green master mix (Life Technologies) and specific primer pairs for each gene (Table 1). Relative expression differences were calculated using the $\Delta\Delta$ CT method and either *Hprt* or *Ppib* as a reference gene.

Table 1: Primers used for quantitative RT-PCR

Primer	Sequence
<i>Dnajc3</i> F	GTGGCATCCAGATAATTTCCAG
<i>Dnajc3</i> R	GAGTTCCAACCTTCTGTGGAAGG
<i>Erdj4</i> F	CTTAGGTGTGCCAAAGTCTGC
<i>Erdj4</i> R	GGCATCCGAGAGTGTTTCATA
<i>Ern1</i> F	CCTGCAACCTTGACTGTTTCC
<i>Ern1</i> R	TCTATTCGGTCACTTACATCCTG
<i>Ero11</i> F	CGGACCAAGTTATGAGTTCCA
<i>Ero11</i> R	TCAGAGAGATTCTGCCCTTCA
<i>Hprt</i> F	TCAGTCAACGGGGGACATAAA
<i>Hprt</i> R	GGGGCTGTACTGCTTAACCAG
<i>Il1b</i> F	GCAACTGTTCCCTGAACTCAACT
<i>Il1b</i> F	ATCTTTTGGGGTCCGTCAACT
<i>Nlrp3</i> F	ATTACCCGCCCGAGAAAGG
<i>Nlrp3</i> R	TCGCAGCAAAGATCCACACAG
<i>Nos2</i> F	CCAAGCCCTCACCTACTTCC
<i>Nos2</i> R	CTCTGAGGGCTGACACAAGG
<i>Ppib</i> F	TGGAAGAGCACCAAGACAGAC
<i>Ppib</i> R	TGCCGGAGTCGACAATGAT
<i>Pycard</i> F	CTTGTCAGGGGATGAACTCAA
<i>Pycard</i> R	GCCATACGACTCCAGATAGTAG
<i>Txnip</i> F	TCAAGGGCCCCTGGGAACATC
<i>Txnip</i> R	GACACTGGTGCCATTAAGTAG
<i>Xbp1^t</i> F	GACAGAGAGTCAAATAACGT
<i>Xbp1^t</i> R	GTCCAGCAGGCAAGAAGGT
<i>Xbp1^s</i> F	AGCTTTTACGGGAGAAAACCTCA
<i>Xbp1^s</i> R	GCCTGCACCTGCTGCG

Luciferase assays: ERAI-Luc BMDCs were seeded onto 96-well plates (7×10^4 cells/well) one day prior to FA treatment. In experiments using pharmacological inhibitors, cells were pretreated with inhibitor alone for 1-3 hours before addition of FAs or other stimuli. After treatment, cells were lysed, and luciferase activity was measured well-by-well following injection of luciferin (GoldBio) using a Mithras luminometer (Berthold) as described (Tomlinson et al., 2004).

Luciferase activities are expressed as fold changes compared to untreated or vehicle-treated cells within the same plate.

Cytokine measurements: Cytokine levels in conditioned media were measured by Ready-Set-Go ELISA kits (Ebioscience). For all IL-1 β secretion measurements, BMDCs were primed with 200 ng/mL LPS (Sigma Aldrich L4391) for 3 hours prior to FA treatment. Pharmacological inhibitors, when used, were present during both priming and treatment periods. ATP (Sigma Aldrich A7699, 5 mM, 45-120 minutes) and nigericin (Calbiochem 481990, 5 μ M, 1 hour) were used as positive controls.

Cell death assays: Caspase-3/7 activity was measured by the EnzChek Caspase-3 Assay Kit (Molecular Probes). Overall cell death was assessed by the ratio of dead cell protease activity to live cell protease activity using fluorogenic substrates from the ApoTox Glo kit (Promega).

Immunoblotting and immunofluorescence: Levels of IRE1 α and PERK phosphorylation were assessed in whole cell lysates (in RIPA buffer with protease and phosphatase inhibitors [Santa Cruz Biotechnology]) using Phos-tag gels as described (Qi et al., 2011). For measurement of ATF6 α , nuclear fractions were obtained by centrifugation. Briefly, cells were detached with trypsin, resuspended in cellular lysis buffer (150 mM NaCl, 20 mM Tris-HCl [pH 7.4], 0.5% Triton X-100, 1 mM PMSF, 100 μ M sodium orthovanadate, 1x protease inhibitor cocktail [Santa Cruz Biotechnology]), and spun at 800 x g for 2 minutes. Pelleted nuclei were then resuspended in nuclear lysis buffer (420 mM NaCl, 20 mM Tris-HCl [pH 8.0], 1.5 mM MgCl₂, 0.2 mM EDTA, 25% glycerol) (Beg et al., 1993), incubated on ice for 30 minutes, and centrifuged at 16,000 x g for 10 minutes. The resulting supernatants were loaded onto 10% SDS-PAGE and transferred onto PVDF membranes (Bio-Rad). Membranes were blocked overnight (4 °C) in

0.1% Tween-20 containing 5% BSA (TBS-T), and after washing, were incubated in TBS-T containing primary antibodies. Membranes were then washed and incubated in TBS-T containing 1:5000 HRP-conjugated anti-rabbit IgG (ECL, GE Healthcare). Immunoreactive bands were detected by chemiluminescence (Super Signal West Pico, Thermo Scientific). For imaging of ASC puncta, BMDCs were replated onto glass coverslips one day prior to stimulation and fixed with 4% PFA in PBS containing 3% sucrose for 10 minutes. Cells were then permeabilized with 0.1% Triton X-100 for 2 minutes, washed with PBS, and blocked with 0.2% BSA, 100mM glycine, and 10% goat serum in PBS for 30 minutes. ASC antibody (1:200 dilution) was incubated for 1 hour followed by a goat anti-rabbit-AF 488 at 1:500. Nuclear staining was performed using DAPI (1 mg/ml) in PBS for 5 minutes. Cells were then mounted with an antifade solution (Vectashield). Images were acquired using the Zeiss Axio Imager 2 apotome upright widefield microscope. Antibodies against IRE1 α (14C10) and PERK (C33E10) were purchased from Cell Signaling; ATF6 α (H-280) and ASC (N-15) antibodies were from Santa Cruz Biotechnology.

In vitro deletion of *Ern1* and expression of mutant IRE1 α : *Ern1*^{fl/fl} and control WT BMDCs were treated with the cell-permeable Cre recombinase HTNC, a His-tagged, TAT-Cre fusion protein with a nuclear localization signal (Excellgen RP-7) as described (Krahmer et al., 2011). *Ern1*^{-/-} MEFs were rescued with full-length human IRE1 α or human IRE1 α lacking its luminal domain (Δ LD-IRE1 α) by retroviral transduction as described (Volmer et al., 2013).

Statistics: Data are represented as mean \pm SD and considered statistically significant at $p < 0.05$. Outliers were removed according to Grubbs' test ($\alpha = 0.05$). Analyses were performed in

GraphPad Prism using two-tailed Student's t test or ANOVA with Holm-Sidak or Dunnett's post-tests in the case of multiple comparisons.

RESULTS

SFA treatment produces a transcriptional signature distinct from LPS treatment and defined by the induction of genes associated with the ER and UPR

We used microarray and functional enrichment analysis to probe the transcriptional response of mouse macrophages to treatment with specific fatty acid (FA) species at a concentration known to reproduce the M_{Me} polarization of ATMs (Kratz et al., 2014). BMDMs were treated for 5 or 20 hours with either the SFA C18:0 stearic acid (SA, 250 μ M) or its monounsaturated counterpart C18:1 oleic acid (OA, 250 μ M) in complex with bovine serum albumin (BSA). Responses captured by microarray were compared to those following a 5-hour treatment with BSA alone (control) or low-dose LPS (1 ng/mL).

LPS treatment resulted in a pro-inflammatory transcriptional signature defined by the up-regulation of 1193 genes, enriched as expected in those encoding factors involved in immune responses, cytokine and chemokine activity, and pattern recognition receptor signaling. However, SA treatment at either time point induced only 8% of the genes induced by LPS (Figure 1A), and additional analyses revealed striking differences between the transcriptional patterns induced by LPS and SA. For example, although biological replicates within conditions were tightly grouped, principal components analysis (PCA) showed each individual treatment condition induced an overall transcriptional response that was unique (Figure 1B). The responses to LPS and SA (20-hour) defined the first two principal components, as they were robustly separated both from the BSA-treated baseline and from each other. The response to OA treatment, by comparison, separated weakly from control along the first two principal components, although somewhat further along the third (Figure 1B). These findings together indicate that whereas OA treatment produces a relatively mild transcriptional response, both SA

and LPS treatments produce strong transcriptional responses that are remarkably different from one another despite the fact that each induces BMDMs to secrete pro-inflammatory cytokines.

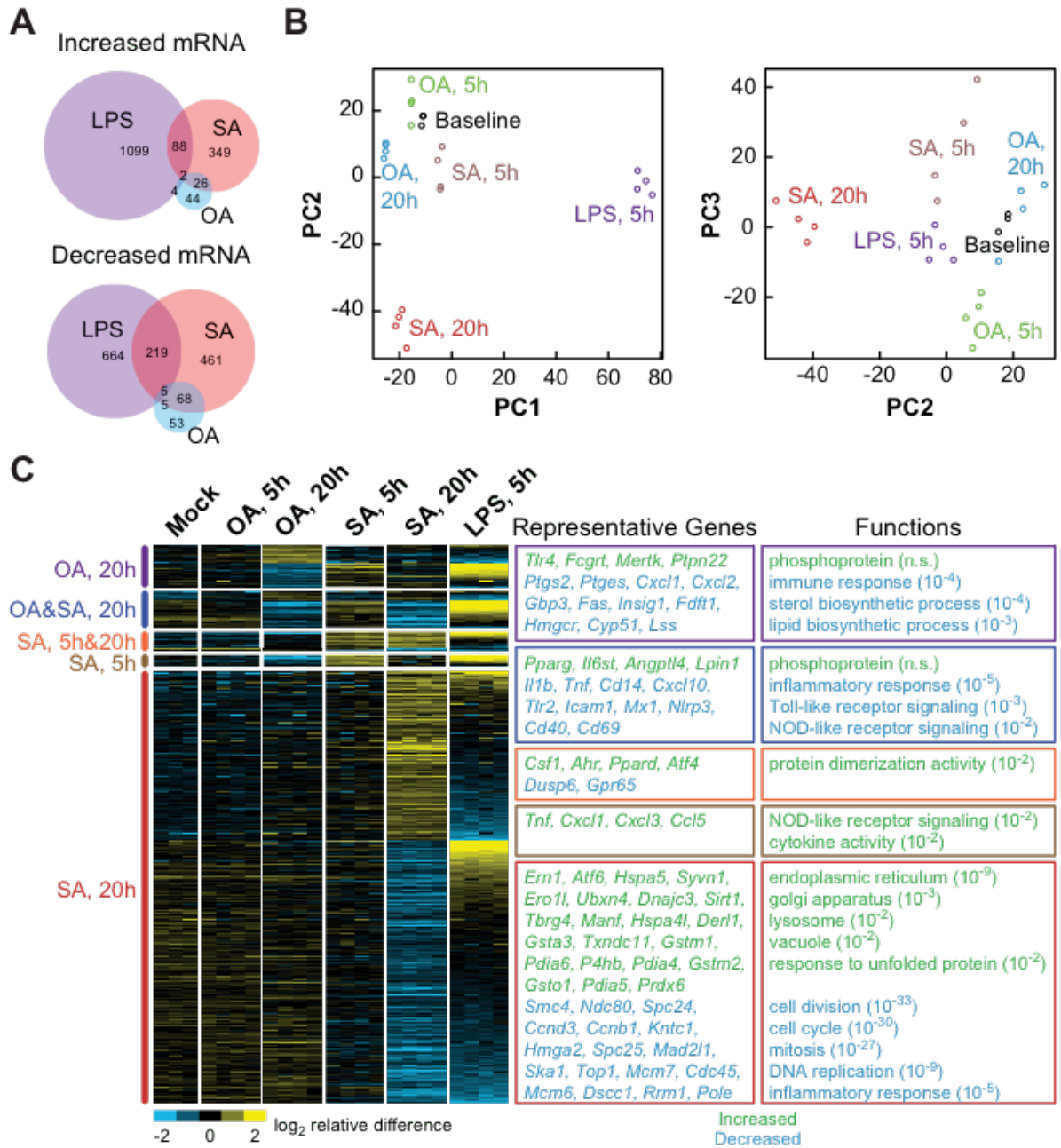


Figure 1. SFA and LPS treatments induce distinct patterns of gene expression in BMDMs

(A) Venn diagrams, depicting the distinct and intersecting nature of gene sets whose transcription is significantly regulated by treatment of BMDMs with LPS (5 h), stearic acid (SA, 5 h or 20 h), or oleic acid (OA, 5 h or 20 h) as compared to baseline vehicle control. (B)

Principal components analysis, showing that the treatment conditions above produce distinct transcriptional responses. Each circle represents one biological replicate of the indicated treatment (n=3-4). (C) Heat map, showing categories of genes significantly up- or down-regulated in response one or more of the treatments (indicated at left). Each column represents one biological replicate of the treatment indicated at the top. Boxes at right show enrichment of functional categories (with Benjamini Hochberg-corrected P values in parentheses) and representative genes that were either significantly increased (green) or decreased (blue) in expression in response to one or more treatments. See also Figure S1.

The distinct responses of BMDMs to FAs and LPS are also clear when significant gene expression differences are grouped and visualized as a heat map (Figure 1C). Functional enrichment analysis showed that although 5 hours of SA treatment up-regulated the expression of genes encoding several chemokines and cytokines, more prolonged SA treatment actually reduced the mRNA levels of genes involved in immune responses and inflammatory pathways. By contrast, the set of 433 genes induced by 20 hours of SA treatment was most profoundly enriched in ER, UPR, Golgi apparatus, and lysosome functional groups, a pattern that was not seen in response to LPS treatment. On the other hand, both LPS and SA (20-hour) treatments reduced the expression of genes involved in functions related to cell division. BMDMs treated with OA for 20 hours had a relatively anti-inflammatory transcriptional profile, as seen in the heat map by an opposing gene expression pattern compared to LPS and down-regulation of genes involved in immune responses (Figure 1C).

The distinction between the transcriptional response of BMDMs to SFA and LPS treatments was further underscored by our analysis of BMDCs lacking Toll-like receptor 4 (TLR4), which binds LPS. On one hand, TLR4 deficiency abolished the ability of both LPS and long-chain SFAs, in this case C16:0 palmitic acid (PA), to increase mRNA levels of the M_{LPS} inflammatory marker *Nos2* (Figure S1A). However, whereas TLR4 deficiency abolished LPS-dependent secretion of the M_{LPS} cytokine TNF, it only minimally reduced PA-induced TNF

secretion (Figure S1B). Furthermore, treating BMDCs with the FA uptake inhibitor sulfo-n-succinimidyl oleate (SSO) markedly reduced PA-induced TNF secretion but did not alter the response to LPS treatment (Figures S1C and D). Taken together, these findings indicate that whereas the LPS-induced inflammatory response of BMDCs is entirely TLR4-dependent, a large component of the low-grade inflammatory response to SFAs is TLR4-independent and instead requires intracellular FA uptake.

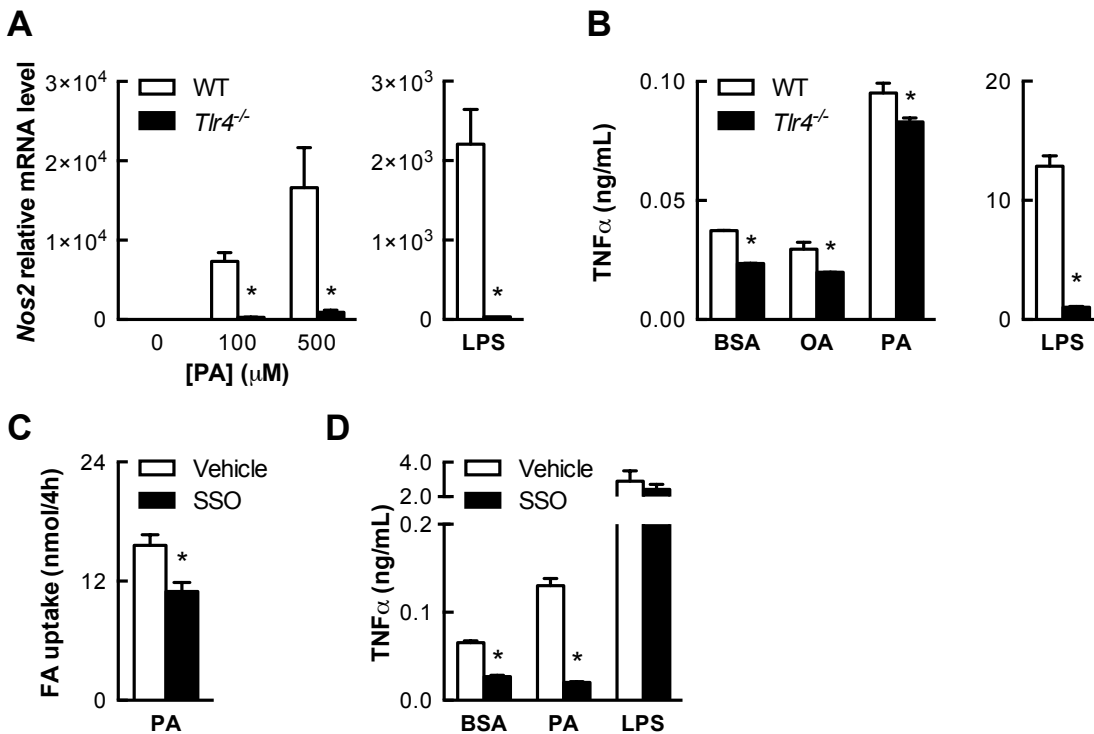


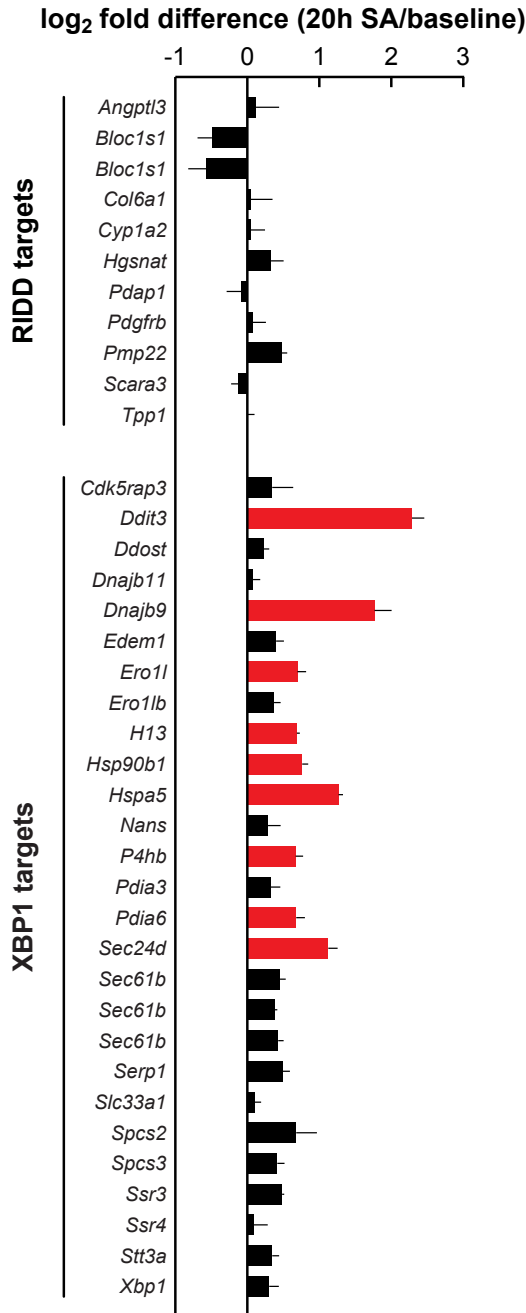
Figure S1 (Related to Figure 1). SFAs and LPS induce inflammatory activation through distinct mechanisms

(A) The M_{LPS} inflammatory marker *Nos2*, measured by quantitative PCR, is up-regulated by treatment with PA (12 h) and LPS (100 ng/mL, 16 h) in wild type BMDCs but not in *Tlr4*^{-/-} BMDCs (n=2-3). (B) TNF secretion stimulated by PA (500 μM, 24 h) is largely intact in *Tlr4*^{-/-} BMDCs, whereas LPS-induced TNF secretion is substantially abrogated by TLR4 deficiency (n=3). (C) Inhibition of ¹⁴C PA uptake by sulfo-n-succinimidyl oleate (SSO, 500 μM, n=6). (D) Abrogation of PA (500 μM)- but not LPS (200 ng/mL)-stimulated TNF secretion by SSO co-treatment (24 h, n=3-4). Error bars, SD. *, p<0.05 vs. WT (A,B) or vehicle (C,D).

SFA treatment preferentially induces adaptive, but not terminal, IRE1 α signaling in both mouse and human macrophages

Consistent with the enrichment of ER and UPR genes in the SA-induced transcriptional signature of BMDMs, we noted upregulation of genes associated with all three arms of the UPR (IRE1 α , PERK, and ATF6), though the ATF6 target genes upregulated by SA were largely shared targets of XBP1. Given the prominence of XBP1 target genes and the induction of IRE1 α itself (*Ern1*) by SA treatment, we asked whether SA preferentially induced either the XBP1-dependent adaptive aspects of IRE1 α signaling, or the IRE1 α -dependent pro-apoptotic RIDD pathway. Genes marking the XBP1-dependent adaptive and RIDD responses, respectively, were compiled from published studies (Acosta-Alvear et al., 2007; A.-H. Lee et al., 2003; So et al., 2012) (Hollien et al., 2009; Maurel et al., 2014; So et al., 2012). Those genes that were identified in at least two of the studies we examined are listed in Figure 2A. Consistent with the reported stimulation of *Xbp1* splicing by SFAs in MCs and other cell types, we found that all probes corresponding to the 25 “consensus” XBP1 target genes were numerically increased in BMDMs treated with SA for 20 hours, and 9 of these genes were significantly up-regulated. By contrast, SA treatment did not significantly decrease the expression of any consensus genes known to be downregulated by the RIDD pathway (Figure 2A).

A



B

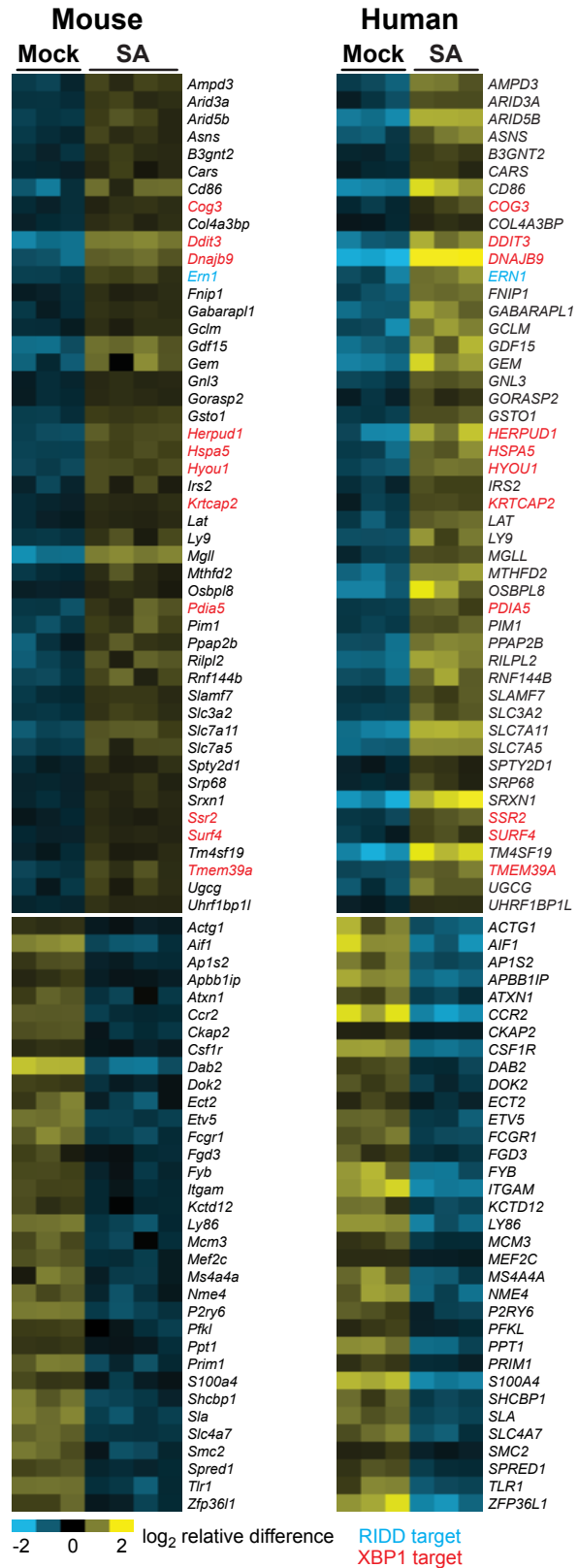


Figure 2. SFA treatment preferentially induces adaptive, but not terminal, IRE1 α signaling in both mouse and human macrophages

(A) Changes in the expression level of genes associated with the adaptive UPR (XBP1 targets) and the terminal UPR (RIDD targets). Differences between the average log₂ expression values for each sample group are shown, with red bars indicating significantly up-regulated genes. Error bars, SD. (B) Heat map, showing the genes significantly up- or down-regulated in response to SA in both mouse BMDMs (this study, 20 h treatment) and human monocyte-derived macrophages (reanalysis of data from Xue, et al. 2014, 24 h treatment). XBP1 targets are shown in red and RIDD targets in blue. See also Figure S2.

In validating our microarray data, we also measured the expression of six RIDD targets by quantitative RT-PCR (qPCR) in BMDCs treated for 4-72 h with a higher dose of SA (500 μ M) or thapsigargin (positive control). Whereas thapsigargin treatment tended to reduce mRNA levels of several of these genes, only one (*Hgsnat*) showed a RIDD-like response to SA treatment (Figure S2A-F). Consistent with this relative lack of RIDD activity, treating BMDCs with 500 μ M PA or SA produced relatively little caspase-3/7 activation or cell death as compared to classical UPR inducers or staurosporine, a pro-apoptotic positive control (Figure S2G and H). Together, these data indicate that SFAs activate predominantly the adaptive components of IRE1 α signaling and suggest that the SFA-induced UPR may not transition to the terminal state that is triggered by the unremitting accumulation of unfolded proteins.

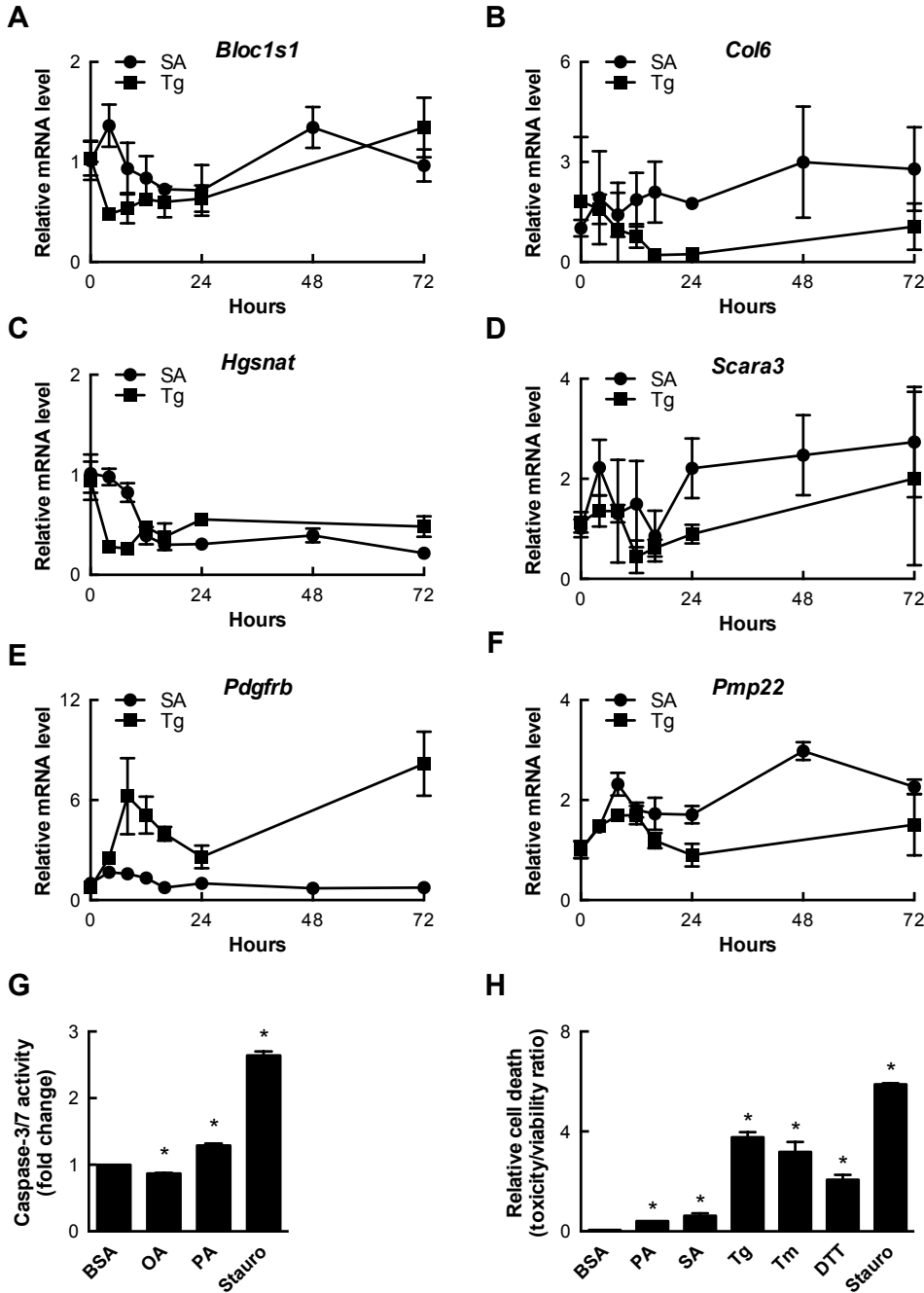


Figure S2 (Related to Figure 2). SFAs do not induce widespread RIDD activation or cell death in BMDCs.

(A-F) mRNA levels of RIDD markers in BMDCs (n=2-3) treated with SA (500 μ M) or thapsigargin (200 nM). (G) Caspase-3/7 activity in BMDCs (n=2) treated with SFAs (500 μ M, 24 h) or staurosporine (1 μ M, 6 h, positive control). (H) Ratio of dead-to-live cell protease activity (measured using fluorescent substrates, n=4) in BMDCs treated with SFAs or staurosporine as in (G) or classical ER stress inducers (200 nM Tg, 5 μ g/mL Tm, 2.5 mM DTT, 24 h). Data in (H) also appear as vehicle condition in Figure 7C. Error bars, SD. *, p<0.05 vs. BSA (G, H).

To test whether the SA-induced IRE1 α -XBP1 macrophage signature we identified is conserved between mice and humans, we performed a meta-analysis comparing the results of our 20-hour SA treatment with those of a published bead-array on SA-treated human monocyte-derived macrophages (Xue et al., 2014). The 48 genes induced by SA in both species, shown in a heat map (Figure 2B), were significantly enriched by genes associated with the ER, including 12 XBP1 targets. By contrast, there were no RIDD-responsive genes downregulated by SA treatment in both species (Figure 2B). Our meta-analysis further confirms that SFA treatment selectively induces adaptive IRE1 α signaling in macrophages, and suggests that this response is prominent in both mice and humans.

IRE1 α is progressively and reversibly activated in mice consuming excess saturated fat

We next examined IRE1 α activation in mice consuming a diet rich in saturated fat. Transgenic mice expressing a luciferase reporter coupled to the IRE1 α -dependent splicing of *Xbp1* (ERAI-Luc; (Iwawaki et al., 2009) were longitudinally monitored while being fed standard chow or a high saturated fat diet (HFD; 42 kcal% fat; 62% saturated). HFD consumption for 1-6 months progressively increased whole-body ERAI-Luc reporter activity compared to age-matched chow-fed mice, with the highest signal intensity coming from the abdomen and proximal lower limbs (Figures 3A and B). ERAI-Luc activity was evident within 5 days of HFD initiation and despite up to 6 months of HFD, was reversible within 5 days of replacing the HFD with standard chow (Figures 3C and D). The changes in reporter activity we observed support the concept that IRE1 α activation in some tissues may be rapidly responsive to changes in dietary fat consumption and not a consequence of obesity *per se*.

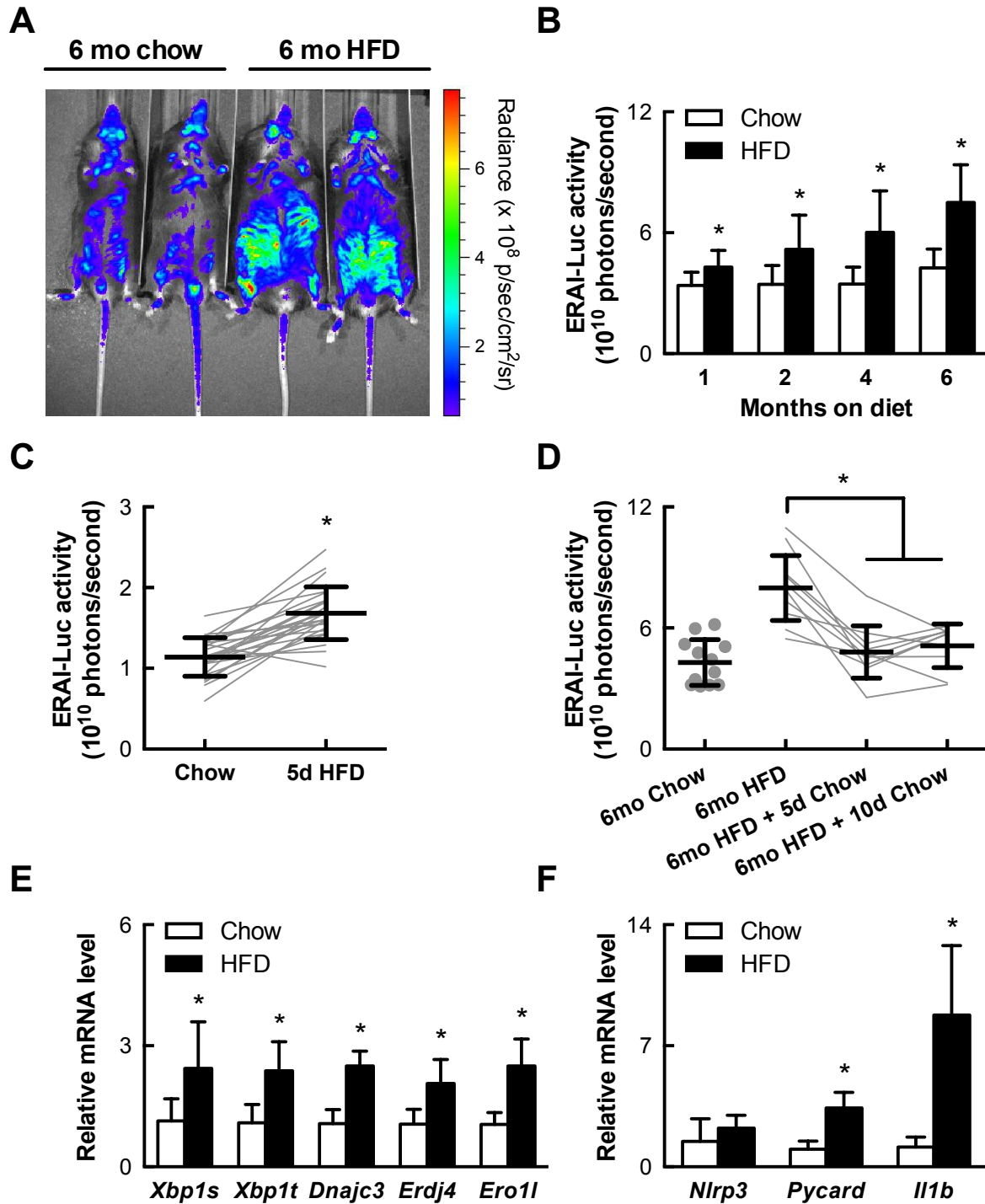


Figure 3. IRE1 α is progressively and reversibly activated in mice consuming excess saturated fat

(A) IRE1 α -mediated *Xbp1* splicing activity as measured by a luciferase reporter (ERA-I-Luc) in live mice fed chow or a high fat diet (HFD) for 6 months (representative images). (B) Quantification of whole-body luciferase activity in ERA-I-Luc mice (n=9-24) fed chow or HFD

and imaged as in (A). (C) Whole-body IRE1 α reporter activity in mice before and after 5 days of HFD (n=24). (D) Reversal of IRE1 α reporter activity in mice switched to chow for 5-10 days after 6 months of HFD. (E) Expression of total and spliced *Xbp1* and XBP1-target genes *Erdj4*, *Ero1l*, and *Dnajc3* as measured by quantitative PCR in the stromal vascular fraction (SVF) of visceral adipose tissue (VAT) of mice fed chow (n=15-18) or HFD for 3 months (n=8-10). (F) Expression of NLRP3 inflammasome-related genes *Il1b*, *Nlrp3*, and *Pycard* in VAT SVF as in (E). Error bars, SD. *, p<0.05 vs. vehicle.

Focusing specifically on the WAT, we found that feeding mice a HFD for 3 months increased the mRNA levels of spliced *Xbp1* and XBP1-dependent target genes in the ATM-containing stromal vascular fraction (SVF) of visceral WAT depots (Figure 3E). Interestingly, HFD-induced XBP1-dependent signaling in SVF cells was concurrent with a significant increase in the mRNA levels of the gene encoding IL-1 β (*Il1b*) and the NLRP3 inflammasome component *Pycard* (Figure 3F). These data suggest that IRE1 α activation in the ATM-rich SVF of HFD-fed mice is accompanied by NLRP3 inflammasome activation, as it is in MCs treated with SFAs *in vitro*.

SFAs act intracellularly to activate IRE1 α and the NLRP3 inflammasome

We examined the mechanism by which SFAs activate IRE1 α in BMDCs from ERAI-Luc mice. PA treatment induced ERAI-Luc reporter activity in a dose- and time-dependent manner, with high PA concentrations producing responses on par with those induced by treatment with the classical UPR activators thapsigargin, dithiotreitol (DTT), and tunicamycin (Figure 4A). Moreover, this response was highly specific to long-chain SFAs (PA and SA) as opposed to medium-chain SFAs or either long-chain monounsaturated or polyunsaturated FAs (Figure 4B). Similar SFA-induced ERAI-Luc reporter responses were seen in BMDMs (Figure S3A).

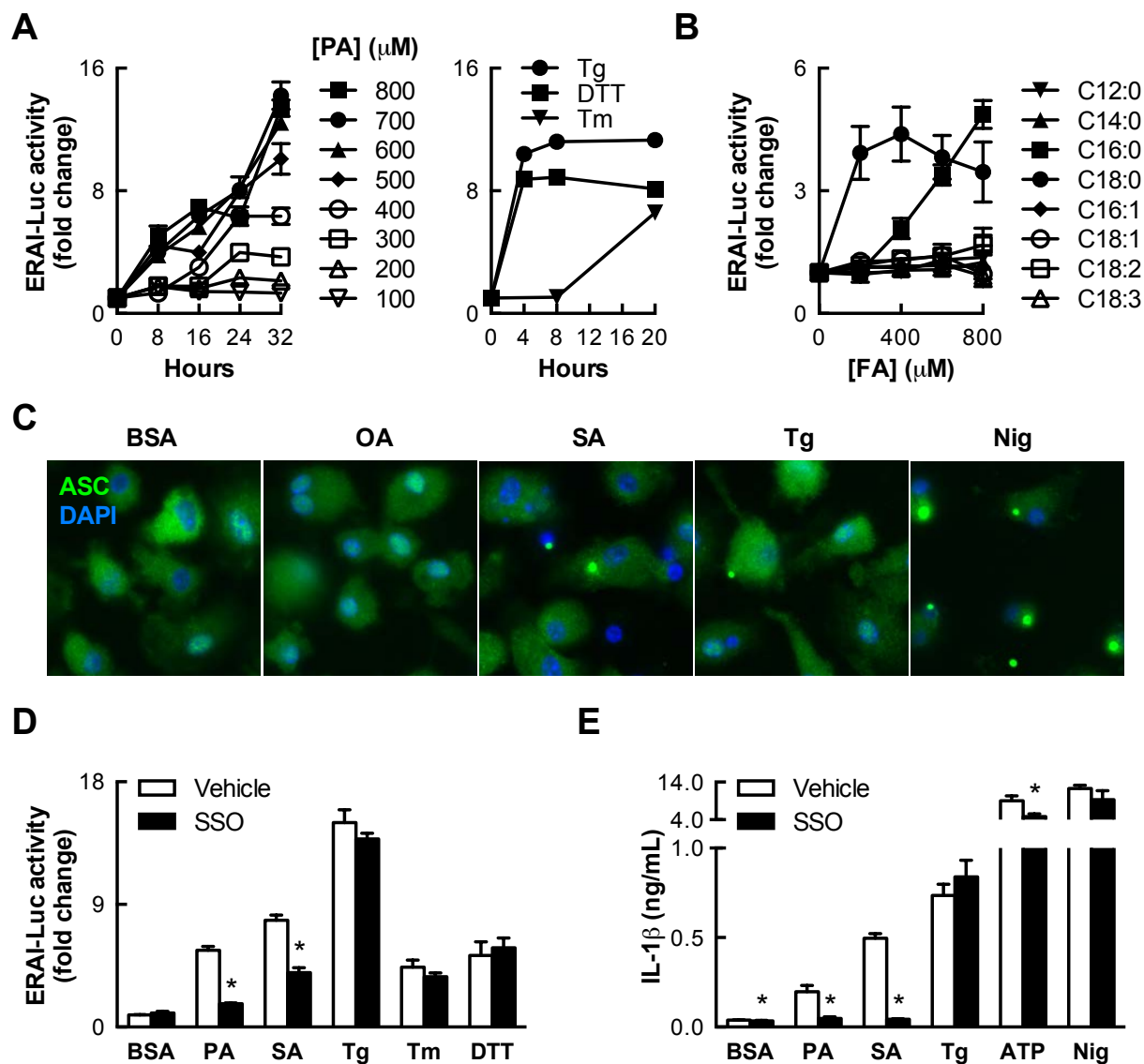


Figure 4. Long-chain SFAs activate IRE1 α and the NLRP3 inflammasome through an intracellular mechanism

(A) Time course of IRE1 α -mediated *Xbp1* splicing activity, as measured by a luciferase reporter in mouse BMDCs (n=2-3) treated with palmitic acid (PA) or the classical ER stress inducers thapsigargin (Tg, 100 nM), dithiothreitol (DTT, 5 mM), and tunicamycin (Tm, 5 μ g/mL). (B) Long-chain SFAs PA (C16:0) and SA (C18:0) specifically induce IRE1 α reporter activity in BMDCs treated for 24 h with a variety of FAs (n=3). (C) Formation of ASC puncta indicative of NLRP3 inflammasome activation in BMDCs treated for 20-24 h with SA (500 μ M), thapsigargin (200 nM), or nigericin (positive control), but not OA (500 μ M) or BSA (vehicle control for FA treatments). (D) Inhibiting FA uptake with sulfo-n-succinimidyl oleate (SSO, 500 μ M) reduces IRE1 α reporter activity (n=6) stimulated by SFAs (1 mM PA, 500 μ M SA) but not classical ER stress inducers (200 nM Tg, 5 μ g/mL Tm, 2.5 mM DTT). (E) SSO specifically abrogates IL-1 β secretion induced by SFAs (500 μ M) but not other stimuli (n=4). In all experiments measuring

IL-1 β secretion, BMDCs were primed with LPS (200 ng/mL, 3 h) prior to stimulation. Error bars, SD. *, $p < 0.05$ vs. vehicle. See also Figure S3.

Building on work showing that SFAs stimulate myeloid cells to secrete IL-1 β , an NLRP3 inflammasome-dependent cytokine (Wen et al., 2011), we found that treating LPS-primed BMDCs with either SA or thapsigargin induced formation of intracellular ASC puncta, indicating inflammasome activation, whereas OA treatment did not do so (Figure 4C). SA and PA, but not OA, also induced NLRP3 inflammasome-dependent IL-1 β secretion in LPS-primed BMDMs (Figure S3B).

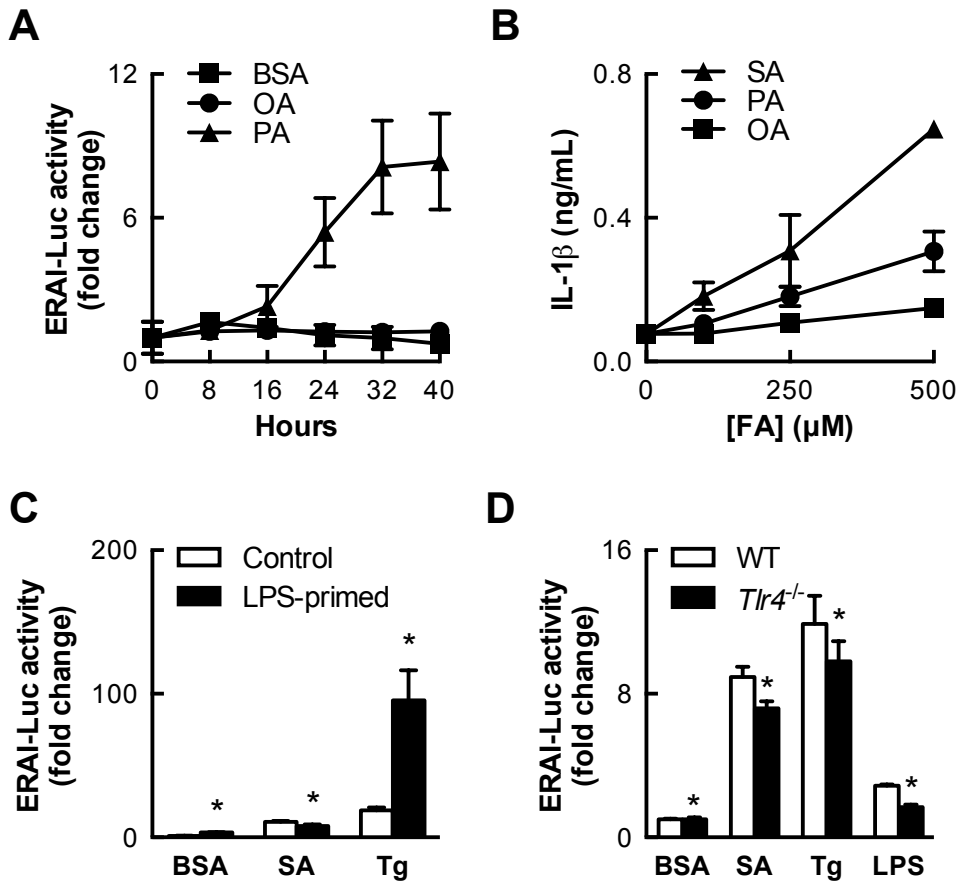


Figure S3 (Related to Figure 4). Responses to SFAs and LPS in BMDMs and BMDCs

(A) Time course of IRE1 α reporter activity in BMDMs treated with FAs (500 μ M, $n=3-4$). (B) IL-1 β secretion by LPS-primed BMDMs treated FAs (24 h, $n=3$). (C) IRE1 α reporter activity in BMDCs ($n=3-5$) treated for 24 h with SA (500 μ M) or Tg (200 nM) with or without LPS priming

(3 h, 200 ng/mL). (D) IRE1 α reporter activity in *Tlr4*^{-/-} BMDCs, showing that the response to LPS treatment is reduced to a greater extent than that to SA treatment (500 μ M, 24 h, n=4-6). Error bars, SD. *, p<0.05 vs. control (C) or WT (D).

On the other hand, LPS priming only minimally impacted SA-induced ERAI-Luc reporter activity (Figure S3C), and LPS treatment alone only modestly stimulated this indicator of *Xbp1* splicing in BMDCs (Figure S3D). Whereas TLR4 deficiency essentially eliminated the capacity of LPS to induce *Xbp1* splicing in BMDCs, it had a much smaller impact on the corresponding response to SA treatment (Figure S3D).

SSO treatment, however, partially abrogated *Xbp1* splicing induced by PA or SA without impacting the responses to classical UPR activators (Figure 4D), indicating that intracellular entry, rather than TLR4, is required for SFAs to induce IRE1 α -dependent *Xbp1* splicing. SSO treatment also abolished IL-1 β secretion from LPS-primed BMDCs stimulated with PA or SA, whereas it did not alter IL-1 β secretion in response to thapsigargin or the canonical NLRP3 inflammasome activators ATP and nigericin (Figure 4E). Treatment with PA or SA was notably insufficient to induce IL-1 β secretion by BMDCs without LPS priming (data not shown), likely due to an inability of SFAs to induce substantial *I1b* transcription on their own.

IRE1 α endoribonuclease activity is required for SFA-induced NLRP3 inflammasome activation

IRE1 α activation has been linked to NLRP3 inflammasome activity in beta cells (Lerner et al., 2012). This, and our finding that intracellular SFAs induce both IRE1 α and NLRP3 inflammasome activation, prompted us to consider whether IRE1 α mediates SFA-induced NLRP3 inflammasome activation in MCs. To test this, we manipulated IRE1 α (*Ern1*) expression by treating BMDCs from mice expressing a conditional allele of *Ern1* (*Ern1*^{fl/fl}) with a cell-

permeable Cre recombinase. This treatment reduced *Ern1* mRNA levels by 63% (Figure 5A) and similarly reduced SFA-induced IL-1 β secretion without altering the response to ATP, which stimulates IL-1 β secretion without inducing ER stress (Figure 5B). We also crossed *Ern1^{fl/fl}* mice with mice that preferentially express Cre in MCs (*Cd11b-Cre*). Primary BMDCs cultured from *Cd11b-Cre⁺/Ern1^{fl/fl}* mice secreted less IL-1 β in response to PA treatment than did similarly treated BMDCs harvested from *Cd11b-Cre⁻/Ern1^{fl/fl}* mice (Figure 5C), although examination of *Ern1* mRNA expression suggested low Cre-LoxP excision efficiency in this model (data not shown). Overall, our findings indicate that IRE1 α is required for SFA treatment to activate the NLRP3 inflammasome.

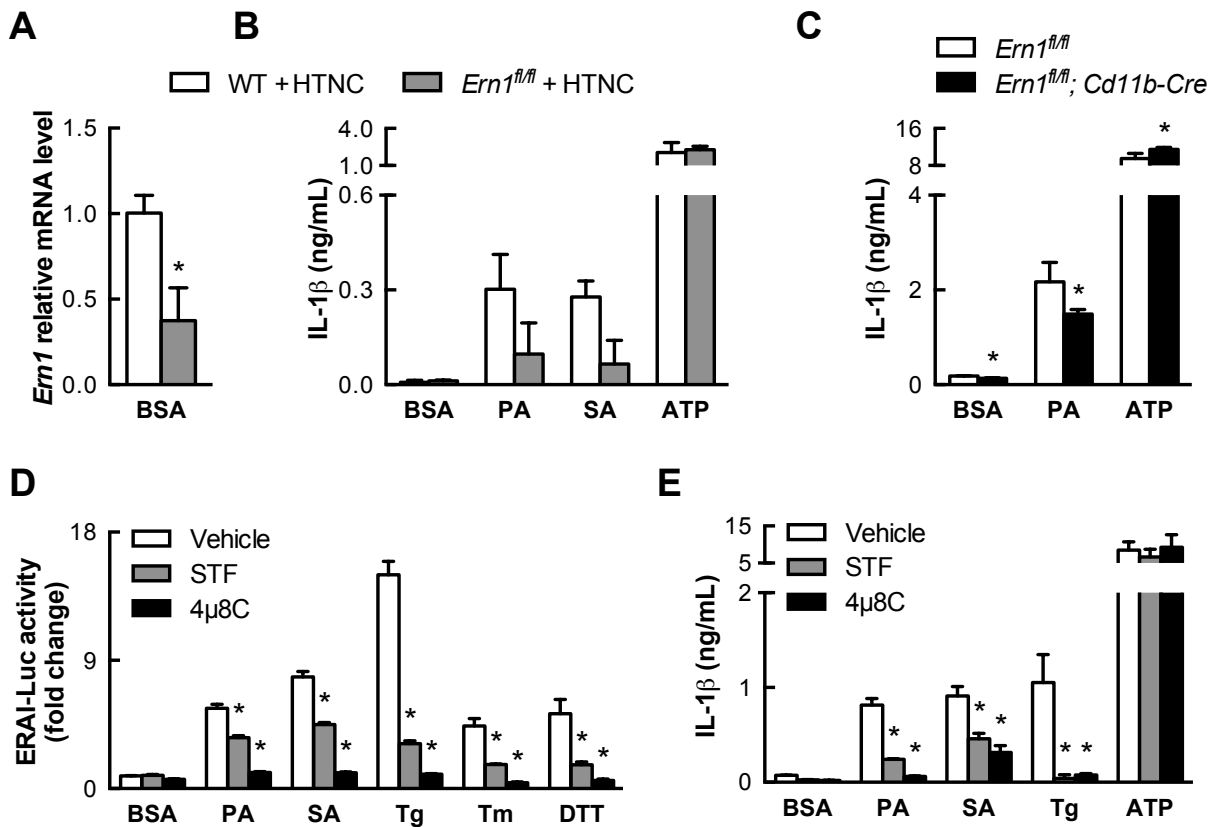


Figure 5. IRE1 α endoribonuclease activity is required for SFA-induced NLRP3 inflammasome activation

(A) Extent of *in vitro* deletion of IRE1 α (*Ern1*) by treating *Ern1^{fl/fl}* BMDCs with the cell-permeable Cre recombinase HTNC, as measured by quantitative PCR (n=3). (B) IRE1 α -deficient

BMDCs from (A) exhibit reduced IL-1 β secretion when stimulated by SFAs (500 μ M, 20 h) but not by ATP (n=2-3). (C) Partial deletion of IRE1 α in *Cd11b-Cre⁺/Ern1^{fl/fl}* BMDCs also modestly diminishes IL-1 β secretion stimulated by PA (500 μ M, 24 h) but not by ATP (n=4). (D) Efficacy of IRE1 α endonuclease inhibitors STF083010 (200 μ M) and 4 μ 8C (50 μ M) in reducing IRE1 α reporter activation by 24 h treatment with PA (1 mM), SA (500 μ M), or classical ER stress inducers (n=6). (E). STF083010 (200 μ M) and 4 μ 8C (200 μ M) abrogate IL-1 β secretion stimulated by SFAs (500 μ M, 24 h) but not ATP (n=3). Error bars, SD. *, p<0.05 vs. WT + HTNC (A,B), *Ern1^{fl/fl}* (C), or vehicle (D,E). See also Figure S4.

IRE1 α is a bifunctional protein with both kinase and endoribonuclease activities. To determine which activity is responsible for NLRP3 inflammasome activation, we treated WT BMDCs with STF083010 and 4 μ 8C, two specific IRE1 α endoribonuclease inhibitors. Remarkably, both inhibitors markedly decreased the extent to which SFA treatment induced either *Xbp1* splicing or consequent IL-1 β secretion (Figures 5D and E). Moreover, they also reduced the ability of other ER stress inducers (e.g. thapsigargin) to activate the NLRP3 inflammasome without altering the ability of ATP to do so. By contrast, treating BMDCs with APY29, which is both an ATP-competitive kinase inhibitor and an allosteric endoribonuclease activator of IRE1 α (L. Wang et al., 2012), failed to reduce SFA-induced IL-1 β secretion and was sufficient to induce IL-1 β secretion on its own (Figure S4A). Thus, the endoribonuclease activity of IRE1 α in MCs specifically mediates NLRP3 inflammasome activation in response to SFAs and other inducers of ER stress.

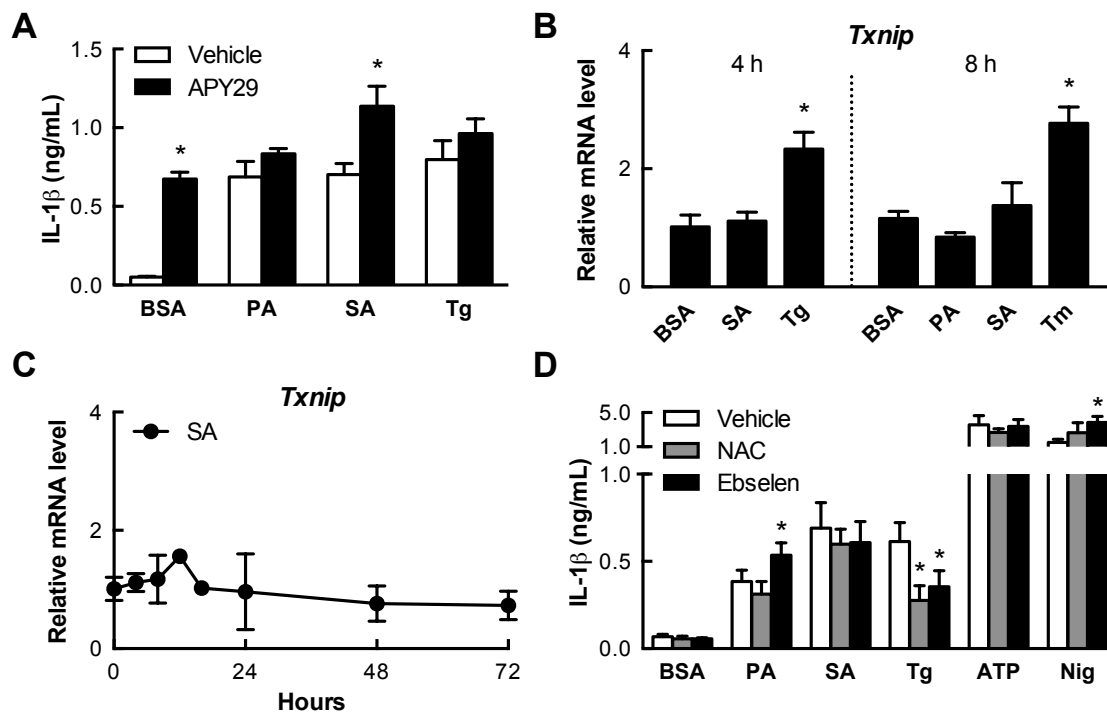


Figure S4 (Related to Figure 5). SFA-induced NLRP3 inflammasome activation does not involve TXNIP induction or ROS

(A) IL-1 β secretion by BMDCs co-treated with APY29 (1 μ M), showing that IRE1 α kinase inhibition and endoribonuclease activation induces IL-1 β secretion on its own and does not diminish that induced by SFAs (500 μ M, 24 h, n=4). (B) Increased mRNA levels of the terminal UPR marker *Txnip*, measured with quantitative PCR, by treatment with thapsigargin (200 nM) and tunicamycin (5 μ g/mL) but not SFAs (500 μ M) in BMDCs (n=3-4). (C) Prolonged SA treatment (500 μ M) does not increase *Txnip* mRNA levels in BMDCs (n=2-3). (D) IL-1 β secretion by BMDCs co-treated with the antioxidants N-acetylcysteine (NAC) and ebselen, showing that antioxidants reduce IL-1 β secretion stimulated by Tg but not SFAs (n=4). Error bars, SD. *, p<0.05 vs. vehicle (A,D) or BSA (B).

Models of ER stress resulting from unfolded protein accumulation showed that IRE1 α promotes the RIDD-dependent induction of TXNIP, which associates with NLRP3 in the presence of reactive oxygen species (ROS) and promotes inflammasome activation (Lerner et al., 2012; Osowski et al., 2012). As predicted by the relative lack of RIDD activity seen in SFA-treated MCs (Figures 2 and S2), *Txnip* mRNA levels in BMDCs were not increased by PA or SA treatment for durations of time over which both thapsigargin and tunicamycin induced *Txnip* to

peak levels (Figure S4B). Indeed, SA did not increase *Txnip* at any point over a 72-hour treatment (Figure S4C). Furthermore, the antioxidants N-acetylcysteine and ebselen reduced IL-1 β secretion in response to treatment with thapsigargin, but not PA or SA (Figure S4D). Our studies focused on TXNIP and ROS together suggest that IRE1 α mediates NLRP3 inflammasome activation by distinct mechanisms when activated by SFAs versus classical UPR activators.

SFAs and classical UPR activators induce Xbp1 splicing by distinct mechanisms

In addition to engaging stimulus-specific downstream effectors of NLRP3 inflammasome activation, we found evidence indicating that SFAs and chemical inducers of ER stress also activate IRE1 α by different mechanisms. In this effort, we studied MCs co-treated with unsaturated fatty acids (UFAs), which can protect many cell types against several effects of SFA exposure (L'homme et al., 2013; Montell et al., 2001; Welters et al., 2004). Co-treating BMDCs with monounsaturated or polyunsaturated UFAs dose-dependently abolished *Xbp1* splicing in response to PA without affecting responsiveness to thapsigargin, tunicamycin, or DTT (Figure 6A). Prolonged pretreatment with OA, even when stopped prior to PA treatment, could reproduce the protective effect of UFA co-treatment, but adding OA to BMDCs after PA treatment was initiated could not reverse *Xbp1* splicing even if the PA was removed from the medium (Figure S5A).

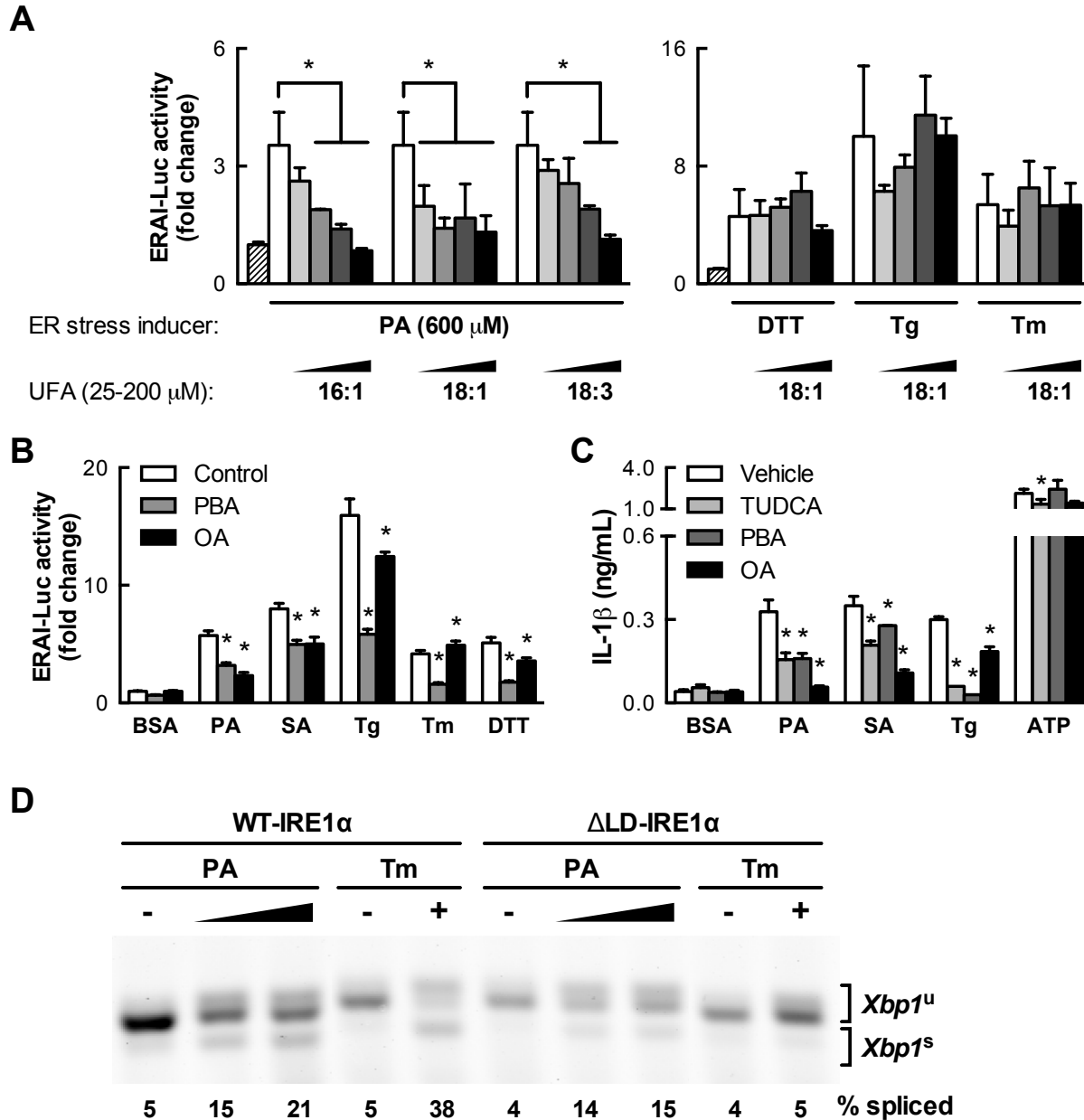


Figure 6. Co-treatment with UFAs specifically mitigates SFA-induced IRE1 α and NLRP3 inflammasome activation

(A) UFA co-treatment of BMDCs dose-dependently reduces IRE1 α reporter activity stimulated by PA but not by classical ER stress inducers (2.5 mM DTT, 100 nM Tg, 5 μ g/mL Tm, 24 h, n=3). (B) In contrast to the SFA-specific protective effect of OA co-treatment (100 μ M, 24 h), co-treatment with the chemical chaperone 4-phenylbutyric acid (PBA, 1 mM) mitigates IRE1 α reporter activity induced by both SFAs (1 mM PA, 500 μ M SA) and classical ER stress inducers (n=6). (C) Reduction of IL-1 β secretion induced by SFAs (500 μ M, 24 h, n=3-4) and other stimuli by co-treatment with the chemical chaperone tauroursodeoxycholic acid (TUDCA, 1 mM), PBA or OA as in (B). (D) *Xbp1* splicing measured by RT-PCR and gel electrophoresis in mouse embryonic fibroblasts expressing only wild type (WT-IRE1 α) or mutant IRE1 α lacking

the luminal domain (Δ LD-IRE1 α) treated with PA (0.5-1 mM) or Tm (5 μ g/ml). PA and Tm lanes were taken from separate sections of the same gel. Error bars, SD. *, $p < 0.05$ vs. control unless otherwise indicated. See also Figures S5, S6, S7, and S8.

The ability of UFAs to block *Xbp1* splicing induced by SFAs but not classical UPR activators suggests that SFAs activate IRE1 α through a mechanism at least partly independent of unfolded protein accumulation. To test this possibility, we treated BMDCs with the chemical chaperones 4-phenylbutyrate (PBA) and tauroursodeoxycholic acid (TUDCA). PBA reduced *Xbp1* splicing induced by classical UPR activators by 62-65% but only diminished SFA-induced *Xbp1* splicing by 38-45% (Figure 6B). Similarly, PBA and TUDCA abolished IL-1 β secretion in response to thapsigargin, but only partially reduced SFA-induced IL-1 β secretion (Figure 6C). Finally, combining PBA or TUDCA with OA co-treatment did not add to the ability of OA to abrogate SFA-induced *Xbp1* splicing or IL-1 β secretion (Figure S5B and C).

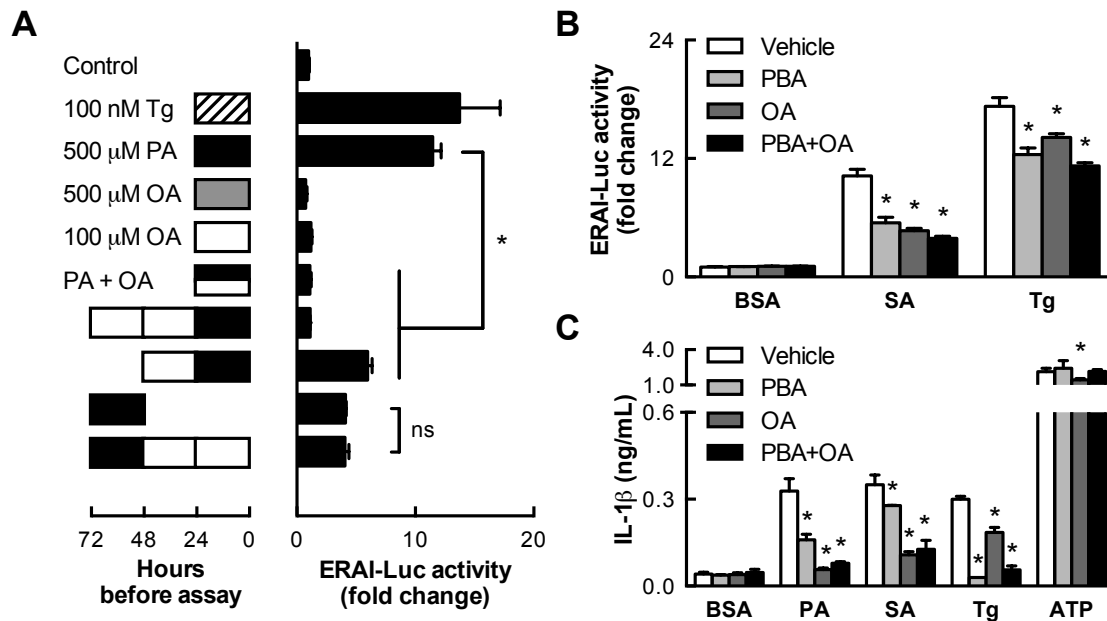


Figure S5 (Related to Figure 6). Combination of PBA and OA does not diminish SFA-induced IRE1 α or NLRP3 inflammasome activation more than PBA or OA alone

(A) Abrogation of PA-induced IRE1 α reporter activity by co-treatment or pretreatment with OA (100 μ M) but not by OA treatment following PA exposure in BMDCs ($n=3$). (B,C) OA (100

μM) and the chemical chaperone PBA (1 mM) both reduce IRE1 α reporter activity (B, n=5-6) and IL-1 β secretion (C, n=4) induced by SFAs (500 μM) or Tg (200 nM) but have no additive effect in combination. Similar findings were obtained using TUDCA (data not shown). (C) Error bars, SD. *, $p < 0.05$ vs. vehicle (B, C) or as indicated.

Together, these data suggest that although SFA treatment may induce some degree of unfolded protein accumulation, SFAs induce IRE1 α activation through a mechanism that is at least partially distinct from that by which unfolded protein accumulation activates IRE1 α . To test this, we built on emerging evidence that IRE1 α can be activated through an ability to sense increases in ER membrane lipid saturation (Volmer et al., 2013). We found that mouse embryonic fibroblasts that only express a mutant form of IRE1 α incapable of recognizing unfolded proteins could still splice *Xbp1* in response to PA treatment, even though their ability to do so in response to tunicamycin was abolished (Figure 6D).

Protein kinase RNA-like endoplasmic reticulum kinase (PERK) is another sensor of ER stress and has also been implicated in membrane lipid sensing (Volmer et al., 2013). Consistently, we found that the kinetics with which SA treatment of BMDCs phosphorylated PERK was similar to those with which it phosphorylated IRE1 α (Figure S6A). By contrast, ATF6 α is an ER stress sensor that has not been implicated in lipid sensing, and we found that SA treatment of BMDCs induced little proteolytic processing or nuclear translocation of ATF6 α (Figure S6B). Taken together, these data support the idea that SFAs can activate IRE1 α and PERK in BMDCs through changes in ER membrane composition but that ATF6 α activation requires unfolded protein accumulation at levels beyond those induced by SFA treatment. Unlike the impact of inhibiting IRE1 α endoribonuclease activity however, PERK inhibition did not reduce SFA-induced IL-1 β secretion (Figure S6C).

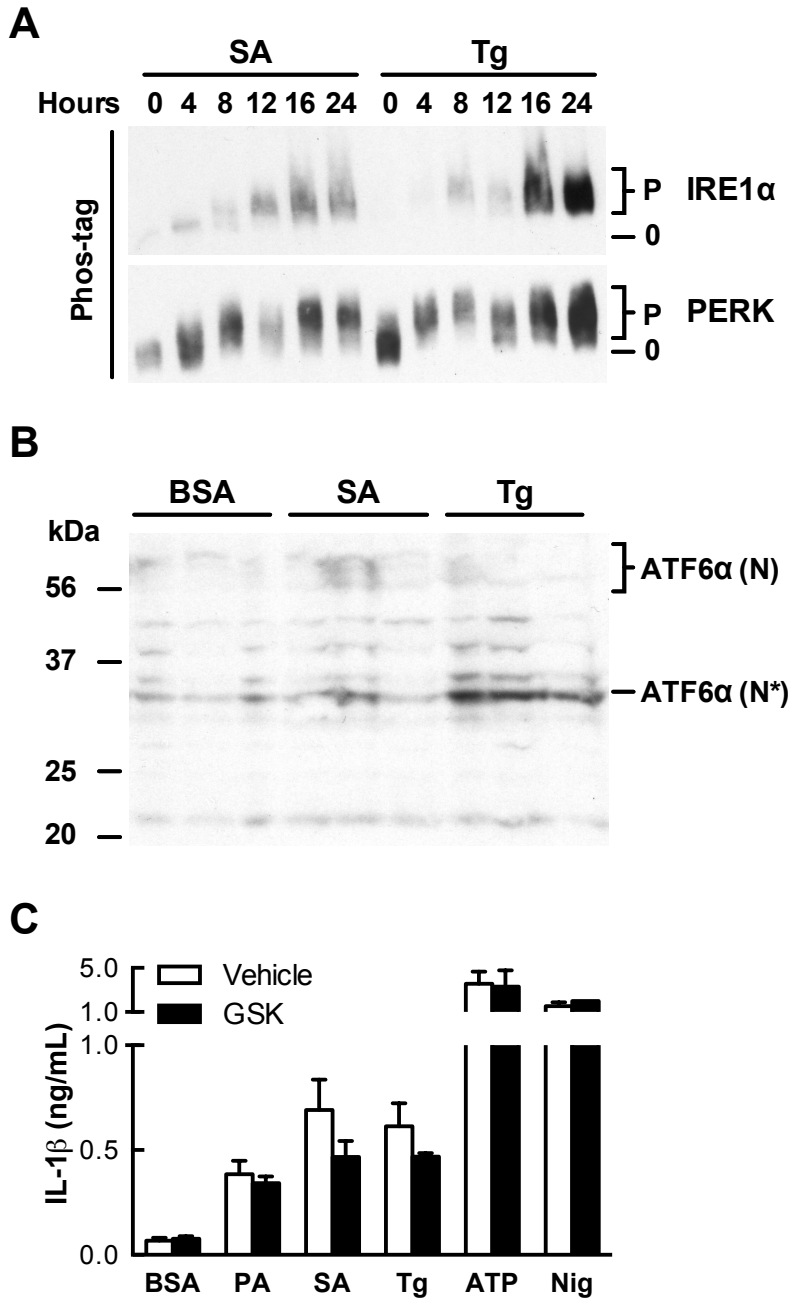


Figure S6 (Related to Figure 6). SA treatment robustly activates IRE1 α and PERK but not ATF6 α

(A) Phosphorylation of IRE1 α and PERK, detected by slower migration through Phos-tag agarose, induced by SA (500 μ M) and Tg (200 nM) in BMDCs. (B) Enrichment of cleaved ATF6 α in nuclear fractions of BMDCs treated for 20 h with Tg but not SA. We detect primarily a ~33 kDa nuclear fragment of ATF6 α (N*); similarly sized fragments have been previously reported and are likely degradation products of the active nuclear form of ATF6 α (N, Thuerlauf et al., 2002). (C) IL-1 β secretion induced by SFAs (500 μ M, 24 h, n=3-4) is not diminished by co-treatment with PERK inhibitor GSK 2656157 (500 nM). Error bars, SD.

Intracellular SFAs flux in a manner that is distinct from UFAs and not controlled by UFA levels

Intracellular UFAs are proposed to mitigate the lipotoxic effects of SFAs by promoting the flux of SFAs into triacylglycerol (TG; (Listenberger et al., 2003), which would potentially reduce their availability to increase ER membrane lipid saturation and thus stimulate IRE1 α activation (Volmer et al., 2013). We treated BMDCs with radiolabeled FAs and found that intracellular OA accumulates preferentially in TG and cholesterol ester storage pools, whereas PA fluxes predominantly into diacylglycerol, phospholipid, and sphingolipid pools (Figures S7A and B). However to our surprise, we did not find that co-treating BMDCs with OA affects the degree to which PA fluxes into TG or any other lipid compartment, precluding the possibility that OA exerts its protective effects in BMDCs by boosting the incorporation of PA into TG (Figures S7C and D).

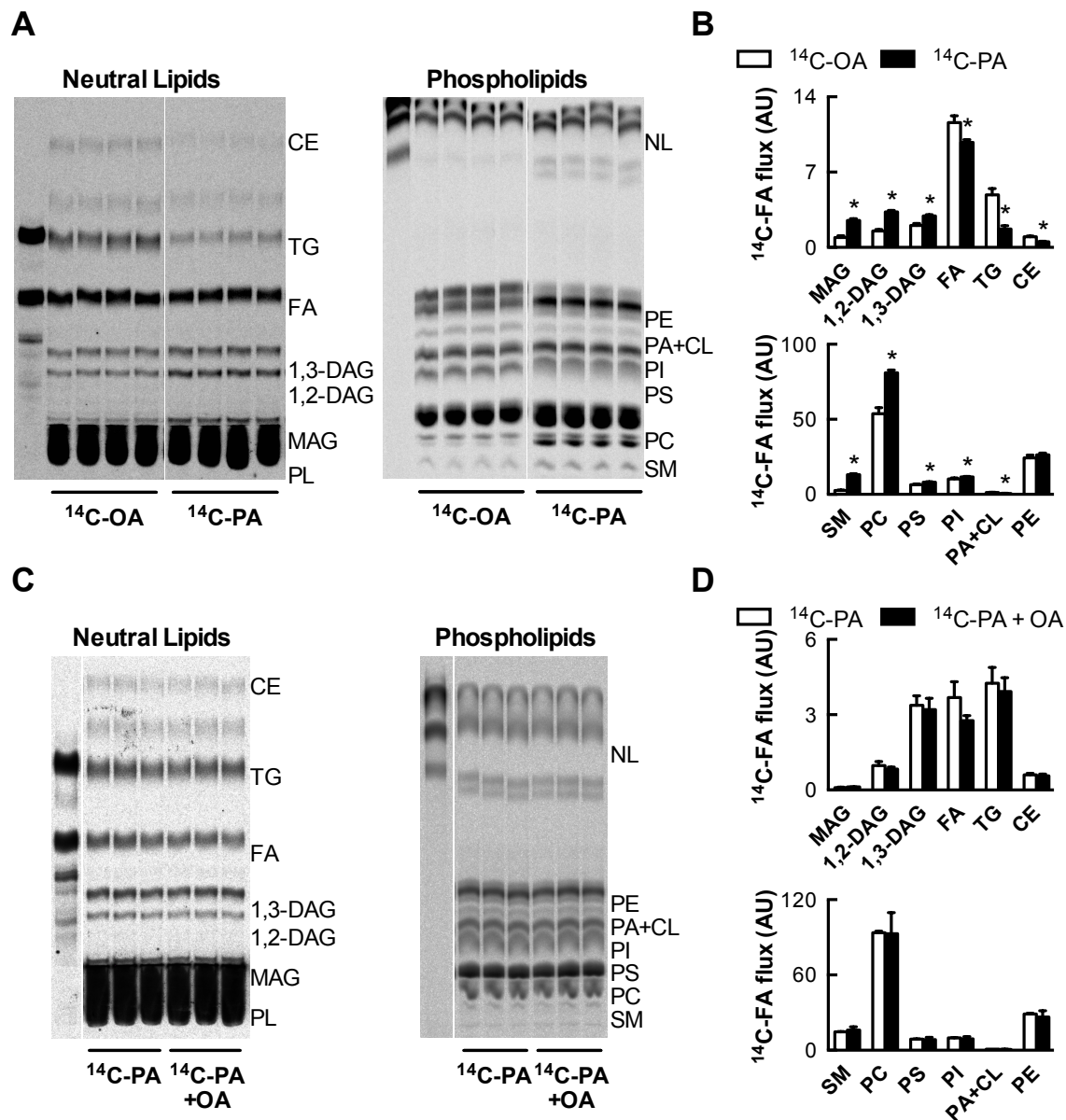


Figure S7 (Related to Figure 6). OA and PA flux to distinct lipid compartments, and OA co-treatment does not modulate the pattern of PA flux

(A) Differential flux of radiolabeled OA and PA into neutral lipid and phospholipid species as determined by TLC and autoradiography. PL, phospholipids; MAG, monoacylglycerol; DAG, diacylglycerol; TG, triacylglycerol; FA, fatty acid; CE, cholesterol ester; SM, sphingomyelin; PC, phosphatidylcholine; PS, phosphatidylserine; PI, phosphatidylinositol; PA+CL, phosphatidic acid and cardiolipin (bands indistinguishable); PE, phosphatidylethanolamine; NL, neutral lipids. $^{14}\text{C-OA}$ and $^{14}\text{C-PA}$ images were taken from separate sections of the same TLC plate (n=4). (B) Quantification of (A). AU, arbitrary units. (C) Lack of change in the flux of radiolabeled PA, measured as in (A), by co-treatment with unlabeled OA (n=3). (D) Quantification of (C). Error bars, SD. *, p<0.05 vs. $^{14}\text{C-OA}$ (B) or $^{14}\text{C-PA}$ (D).

Furthermore, altering the capacity of macrophages to form TG had little impact on the ability of SFA treatment to activate either IRE1 α or the NLRP3 inflammasome. For example, BMDCs from WT mice lacking the TG-synthetic enzyme DGAT1 (*Dgat1*^{-/-}), or transgenic mice overexpressing DGAT1 in MCs (*aP2-Dgat1*) did not substantially differ in their vulnerability to SFA-induced *Xbp1* splicing (Figure S8A). Moreover, neither genetic deficiency nor pharmacologic inhibition of DGAT1 could impair either the capacity of SFA treatment to induce IL-1 β secretion or the protective effects of OA in SFA-treated BMDCs (Figures S8B-E). These findings support the concept that rather than altering the flux of SFAs into TG, the ability of UFAs to protect against SFA-induced IRE1 α activation and subsequent NLRP3 inflammasome activation is a function of their own flux into phospholipids or other lipid species that may counteract SFA-induced changes in membrane lipid composition and saturation.

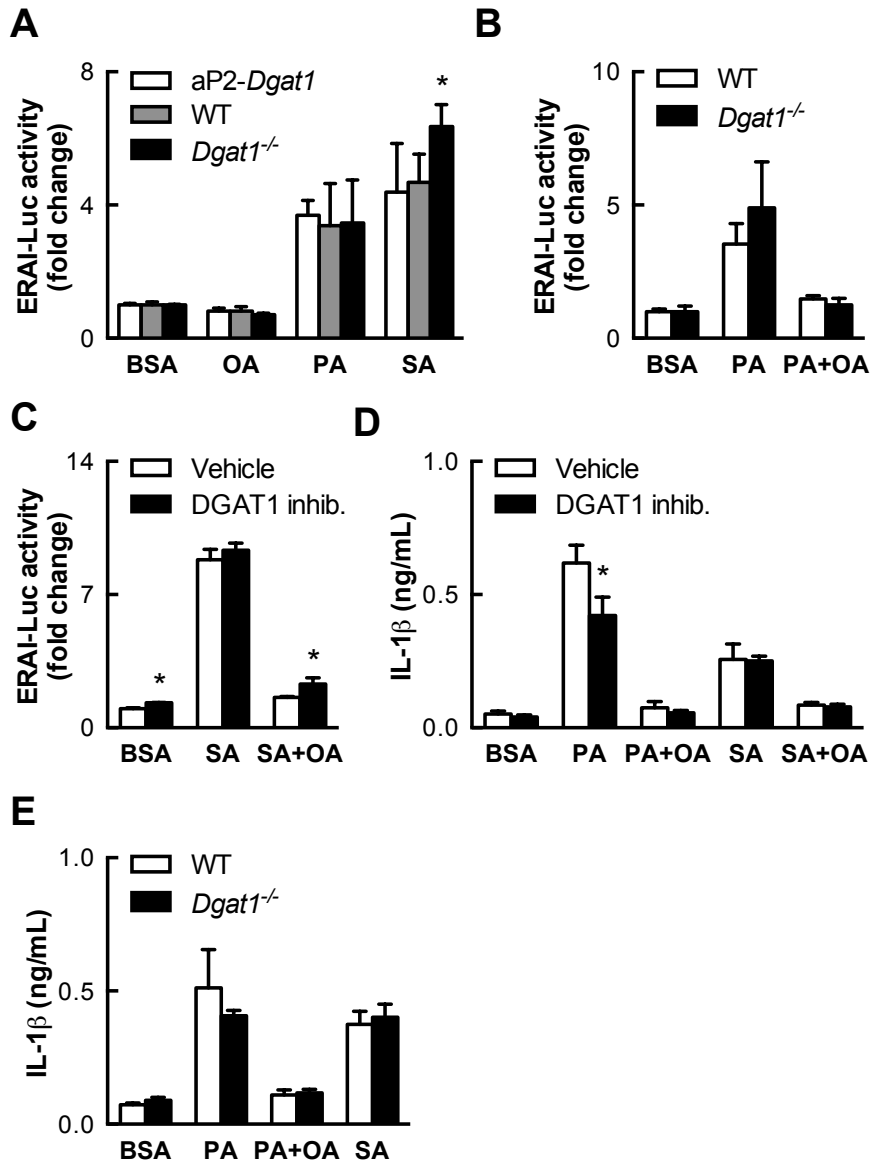


Figure S8 (Related to Figure 6). DGAT1 activity does not control SFA-induced IRE1 α or NLRP3 inflammasome activation

(A) IRE1 α reporter activity, showing that the response to SFAs (400 μ M, 24 h) is largely unchanged in BMDCs lacking (*Dgat1*^{-/-}) or overexpressing (*aP2-Dgat1*) the triacylglycerol synthesis enzyme DGAT1. (B) IRE1 α reporter activity in *Dgat1*^{-/-} BMDCs, showing retention of the ability of OA co-treatment (100 μ M) to abrogate reporter activity induced by PA (600 μ M, 24 h). (C) Inhibition of DGAT1 does not affect IRE1 α reporter activation by SA (500 μ M, 24 h) or the protective effect of OA co-treatment (100 μ M). (D) IL-1 β secretion by BMDCs, showing that DGAT1 inhibition modestly reduces IL-1 β secretion induced by PA but not SA (500 μ M, 24 h) and does not affect protection by OA co-treatment (100 μ M). (E) IL-1 β secretion in response to SFAs (500 μ M, 24 h) and the impact of OA co-treatment (100 μ M) are unaltered in *Dgat1*^{-/-} BMDCs. n=4 for all treatments. Error bars, SD. *, p<0.05 vs. WT (A,B,E) or vehicle (C,D).

The flux of SFAs into phosphatidylcholine contributes to IRE1 α and NLRP3 inflammasome activation

If SFA-induced IRE1 α activation is a function of effects on ER membrane lipid composition and saturation, as our data suggests, then blocking the flux of SFAs into membrane lipids such as phospholipids and sphingolipids should mitigate IRE1 α activation and resultant NLRP3 inflammasome activation. Indeed, inhibiting the first step of de novo sphingolipid and ceramide synthesis with myriocin was shown to reduce IL-1 β secretion in macrophages co-treated with PA and LPS (Schilling et al., 2012). However, more recent work has called this mechanism into question (Camell et al., 2015), and we observed that myriocin treatment did not significantly reduce IRE1 α activation or IL-1 β secretion in response to PA (Figure S9A and B).

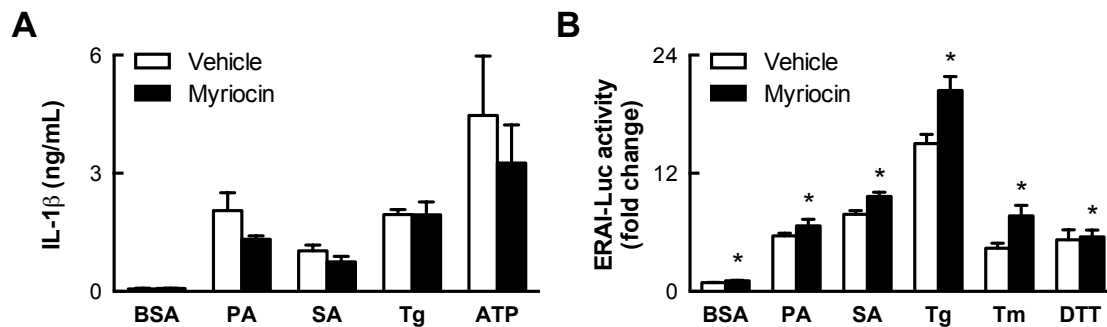


Figure S9 (Related to Figure 7). Limiting the flux of SFAs into sphingolipids does not reduce SFA-induced IRE1 α or NLRP3 inflammasome activation

(A) IL-1 β secretion by BMDCs, showing a modest trend toward reduction of SFA (500 μ M, 24 h)-induced, but not Tg or ATP-induced IL-1 β secretion by the sphingolipid biosynthesis inhibitor myriocin (n=4). (B) Lack of impact of myriocin on the ability of SFAs (1 mM PA, 500 μ M SA, 24 h) or classical ER stress inducers to stimulate IRE1 α reporter activity (n=6). Error bars, SD. *, p<0.05 vs. vehicle.

Phosphatidylcholine (PC) is the most abundant phospholipid in mammalian cellular membranes, including those of the ER, and we saw that BMDCs form PC to a greater degree

upon treatment with PA than OA (Figures S7A and B). As such, we sought to determine the impact of limiting PC synthesis in BMDCs treated with SFAs. The synthetic alkylphospholipids miltefosine and edelfosine inhibit CDP:phosphocholine cytidylyltransferase (CCT), which catalyzes the rate-limiting step of PC biosynthesis. Treatment with either miltefosine or edelfosine reduced the ability of both PA and SA to induce *Xbp1* splicing and IL-1 β secretion, suggesting that incorporation of SFAs into PC contributes to the activation of IRE1 α (Figures 7A and B).

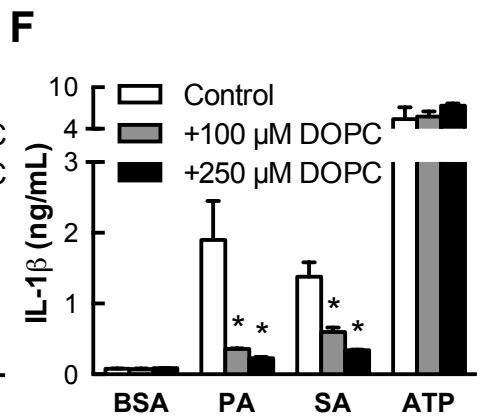
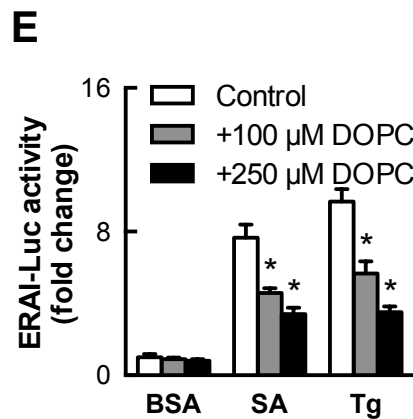
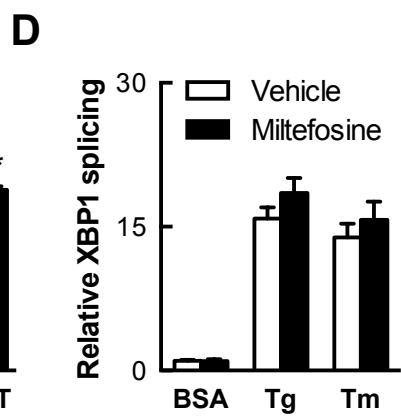
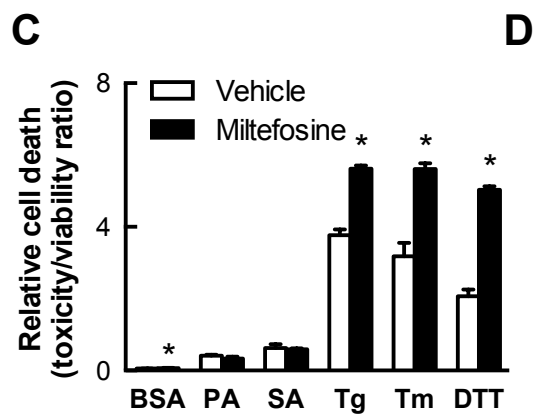
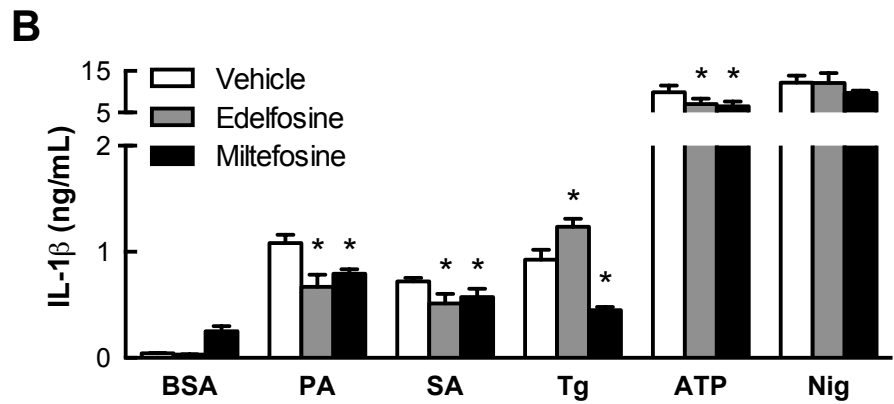
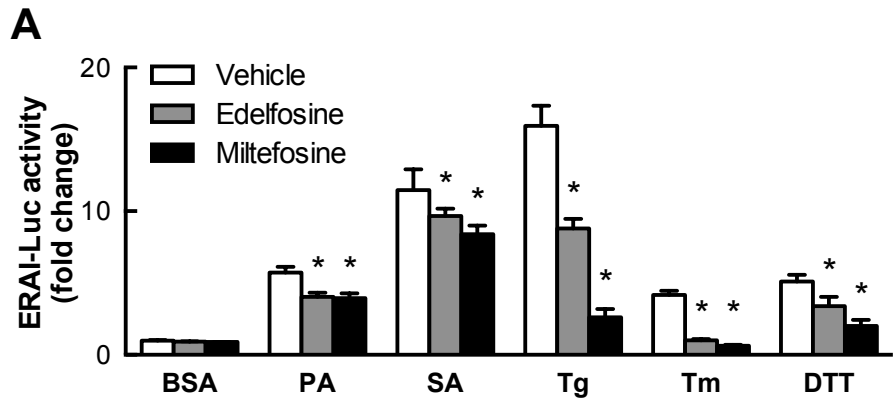


Figure 7. Limiting the ability of SFA treatment to increase phospholipid saturation blocks consequent IRE1 α and NLRP3 inflammasome activation

(A) Phosphatidylcholine biosynthesis inhibitors edelfosine (25 μ M) and miltefosine (100 μ M) reduce IRE1 α reporter activity induced by SFAs (1 mM PA, 500 μ M SA, 24 h, n=6). (B) Edelfosine and miltefosine co-treatment as in (A) diminishes IL-1 β secretion induced by SFAs (500 μ M, 24 h, n=4). (C) Miltefosine co-treatment potentiates cell death due to classical ER stress inducers but not SFAs (500 μ M, 24 h, n=4). (D) Tg- and Tm-induced *Xbp1* splicing is unaffected by miltefosine co-treatment when measured by quantitative PCR (n=4), indicating that reductions in IRE1 α reporter activity in BMDCs co-treated with inhibitors and classical ER stress inducers in (A) are secondary to cell death. (E) Reduction of SA- and Tg-induced IRE1 α reporter activity in BMDCs co-treated with dioleoylphosphatidylcholine (DOPC) liposomes for 24 h (n=5). (F) Abrogation of SFA-induced, but not ATP-induced, IL-1 β secretion by DOPC co-treatment of BMDCs (n=3-4) as in (E). Error bars, SD. *, p<0.05 vs. vehicle (A-D) or control (E,F). See also Figure S9.

Interestingly, whereas CCT inhibition was tolerated by untreated BMDCs and those treated with SFAs, it caused pervasive cell death and reduced ERAI-Luc reporter activity in cells treated with thapsigargin, tunicamycin, or DTT (Figure 7A and C). Moreover unlike its effect on SFA treatment, miltefosine did not reduce *Xbp1* splicing induced by thapsigargin and tunicamycin when measured by qPCR (Figure 7D). This finding suggests that the miltefosine-induced reduction in ERAI-Luc reporter activity seen in the context of severe unfold protein accumulation is secondary to cell death and highlights the potential importance of PC biosynthesis in the ability of BMDCs to contend with ER stress under such conditions.

Our findings support the concept that SFA flux into PC leads to IRE1 α activation and that UFAs counteract this activation through their own flux into phospholipids. We therefore reasoned that enriching MC membranes with unsaturated PC would be sufficient to reproduce the protective effects of UFA co-treatment. BMDCs were co-treated with SFAs and liposomes composed of dioleoylphosphatidylcholine (DOPC). Remarkably, DOPC liposomes (100-250 μ M) abrogated SA-induced *Xbp1* splicing (Figure 7E) to a degree similar to that observed with OA co-treatment at comparable concentrations (Figure 6B and C) and also reduced *Xbp1*

splicing in response to thapsigargin (Figure 7E). Together these data strongly support the concept that reducing the saturation status of membrane phospholipids prevents activation of IRE1 α by SFA excess and decreases the sensitivity of IRE1 α to unfolded protein accumulation.

Importantly, and in correspondence with their effect on limiting IRE1 α activation, DOPC liposomes also protected against IL-1 β secretion induced by SFAs or thapsigargin but not by ATP (Figure 7F). Thus, shifting the equilibrium of cellular phospholipids to favor higher unsaturation specifically abolishes the ability of SFAs to induce IL-1 β secretion without impairing the responsiveness to DAMPs that are indicative of infection or tissue damage.

Summary

Diets rich in saturated fatty acids (SFAs) produce a form of tissue inflammation driven by “metabolically activated” macrophages. We show that excess SFAs induce a unique transcriptional signature in both mouse and human macrophages that is enriched by a subset of ER stress markers, particularly IRE1 α and many adaptive downstream target genes (Figure 8). SFAs also activate the NLRP3 inflammasome in macrophages, resulting in IL-1 β secretion. We found that IRE1 α mediates SFA-induced IL-1 β secretion by macrophages, and that its activation by SFAs does not rely on unfolded protein sensing. We show instead that the ability of SFAs to stimulate either IRE1 α activation or IL-1 β secretion can be specifically reduced by preventing their flux into phosphatidylcholine (PC) or by increasing unsaturated PC levels. IRE1 α is thus an unrecognized intracellular PC sensor critical to the process by which SFAs stimulate macrophages to secrete IL-1 β , a driver of diet-induced tissue inflammation.

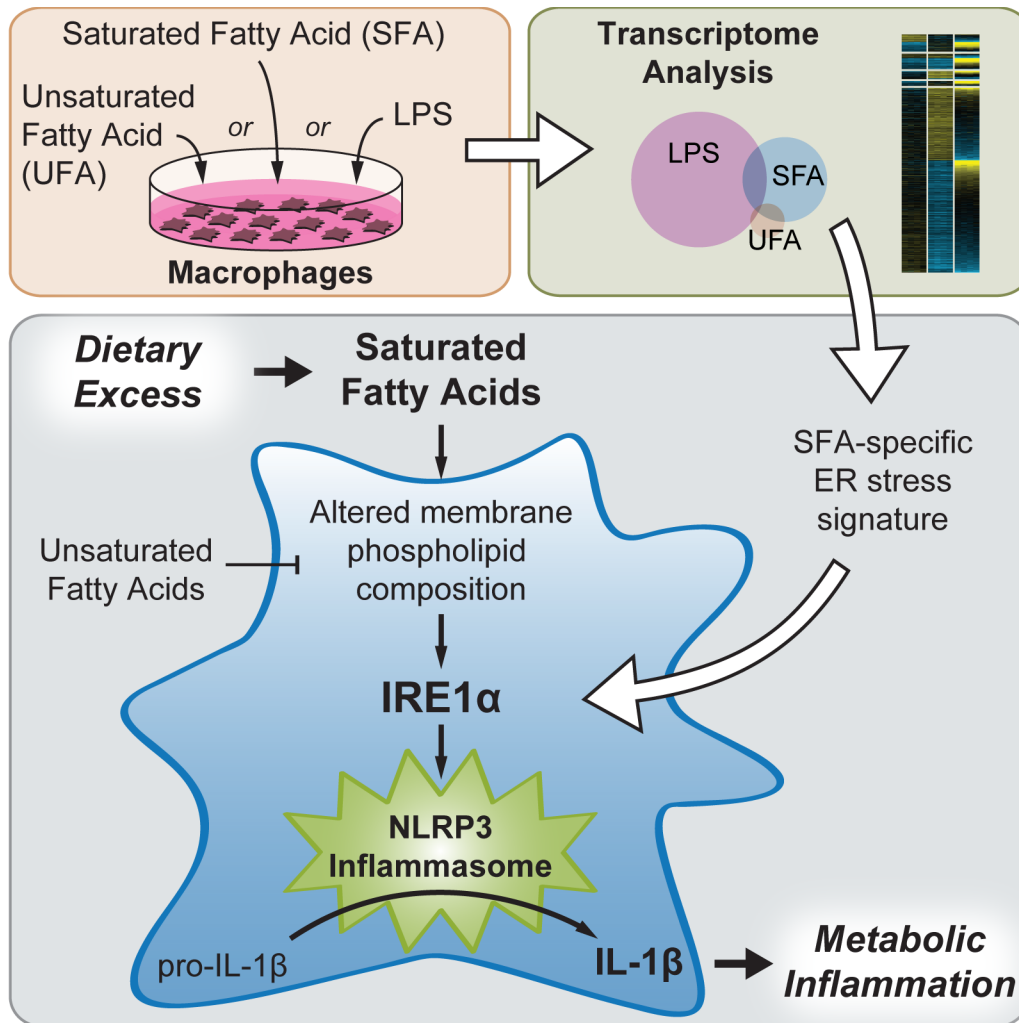


Figure 8: Model depicting activation of IRE1 α and the NLRP3 inflammasome by SFAs in macrophages.

DISCUSSION

Although ATMs chronically activated by DIO share features in common with macrophages responding acutely to pathogens, such as secretion of pro-inflammatory cytokines, key distinctions exist that could potentially be exploited therapeutically to combat inflammation-related metabolic dysfunction. Here we show that macrophages activated by SFA treatment display a pronounced transcriptional signature of ER stress, in striking contrast to the inflammatory signature induced by stimulation with LPS. This ER stress response, driven by the flux of SFAs to PC and resultant IRE1 α activation, has functional consequences. In particular, we found that SFA-induced IRE1 α endoribonuclease activity mediates activation of the NLRP3 inflammasome and secretion of IL-1 β , a pro-inflammatory cytokine associated with insulin resistance. These findings were corroborated *in vivo*, as we could progressively increase tissue IRE1 α activity by feeding mice a diet high in saturated fat. Indeed, such a diet activated both IRE1 α and the NLRP3 inflammasome in the ATM-rich compartment of the WAT. Thus, IRE1 α activation among tissue MCs may be important in promoting inflammation and metabolic disease in DIO.

SFAs are thought to elicit pro-inflammatory TLR4 signaling in MCs on account of their similarity to the saturated acyl chains of LPS (J. Y. Lee et al., 2001; Suganami et al., 2007), which bind specifically to TLR4 (Park et al., 2009). However, direct binding of SFAs to TLR4 has never been demonstrated (Schaeffler et al., 2009), though an adaptor protein, Fetuin A, has been proposed (Pal et al., 2012). It has become increasingly clear that SFAs do not merely mimic LPS (Erridge and Samani, 2009; Kratz et al., 2014; Xu et al., 2013), and our microarray analysis underscores this point. Short-term treatment of BMDMs with SA resulted in relatively little alteration in gene expression compared to the robust induction of inflammatory and immune

response genes in response to LPS treatment of the same duration, and more prolonged SA treatment produced a distinct transcriptional signature from that of LPS. Though SFAs do stimulate M_{LPS} inflammatory pathways and the secretion of associated cytokines such as TNF from BMDCs, the magnitude of this response is small compared to that induced by LPS or other PAMPs, and SFAs are insufficient to substitute for LPS in priming the NLRP3 inflammasome. Furthermore, we found that many of the responses to SFA treatment are independent of TLR4 and instead require FA uptake, suggesting that additional intracellular pathways mediate SFA-induced macrophage activation.

Indeed, we demonstrate that activation of IRE1 α via the flux of SFAs into phospholipids and resulting induction of the UPR are defining features of MC activation by SFAs. Previous transcriptional and proteomic analyses of macrophages treated with SFAs have revealed programs of lysosomal biogenesis and intracellular lipid metabolism (Kratz et al., 2014; Xu et al., 2013), but a predominant ER stress signature has not been described. Differences in methodology may account for these varying results. Nonetheless, our meta-analysis against SA-treated human macrophages supports our findings in mouse MCs and suggests that activation of IRE1 α by SFAs is a conserved process.

Our transcriptome analysis also reveals that SFA treatment disproportionately induces the XBP1-dependent adaptive arm of IRE1 α signaling. Despite stimulating robust IRE1 α activation, evidenced by similar levels of *Xbp1* splicing to those elicited by thapsigargin and other UPR inducers, SFA treatment does not result in an extensive RIDD response. This bias towards adaptive IRE1 α signaling may outweigh the pro-apoptotic pathways associated with the PERK arm of the UPR, as we observed little apoptosis or cell death in BMDCs treated with SFAs despite a significant level of PERK phosphorylation.

In models of prolonged or irremediable ER stress due to unfolded protein accumulation, IRE1 α undergoes a “switch” from adaptive to terminal signaling outputs, which is mediated by a transition to higher-order oligomerization of IRE1 α that promotes RIDD (reviewed by (Maly and Papa, 2014). Our results lead us to speculate that activation of IRE1 α in response SFAs does not lead to extensive oligomerization of IRE1 α . Consistent with this hypothesis, SFA-treated cells expressing fluorescently tagged IRE1 α do not form the large IRE1 α oligomeric puncta that are seen following treatment with classical ER stress inducers (Kitai et al., 2013). Thus, SFA treatment may represent a paradigm in which progressive, dose-dependent *Xbp1* splicing does not trigger the typical switch-like behavior of IRE1 α . This SFA-induced mode of IRE1 α activation appears to mediate NLRP3 inflammasome activation by a different mechanism than that which does so under conditions of excess unfolded proteins, and the molecular features defining this mechanism need to be explored. Based on this, our data suggest that disrupting either *Xbp1* splicing or XBP1-dependent transcriptional activity may reveal new ways to control NLRP3 inflammasome activation in the context of SFA excess and should be a focus of future studies.

Though IRE1 α is best known as a sensor of unfolded proteins, its ability to directly sense changes in membrane lipid composition in mammalian cells was recently appreciated (reviewed by Volmer and Ron, 2015). This ability of IRE1 α to recognize and respond to ER membrane perturbations may be critically linked to its role in regulating lipid homeostasis. Activation of IRE1 α promotes phospholipid synthesis in order to expand the capacity of the ER during times of increased protein folding demand. The importance of this adaptive response for cell survival was strikingly evident in our studies, as BMDCs in which PC biosynthesis was pharmacologically impaired did not survive treatment with classical ER stress inducers. By

contrast, inhibiting PC biosynthesis did not cause such cell death in response to SFA treatment, suggesting that the unfolded protein burden associated with SFA-stimulated IRE1 α activation does not necessitate ER expansion to the degree that is required following treatment with traditional UPR inducers.

Though we clearly show that the ability of IRE1 α to recognize unfolded proteins is not needed for its activation by SFAs, we cannot completely rule out the possibility that unfolded proteins may play some role in this process. For example, many chaperones that facilitate protein folding require calcium, which is depleted from the ER following SFA exposure (Cunha et al., 2008; Egnatchik et al., 2014; Wei et al., 2009). ER luminal calcium levels are maintained by the sarco/endoplasmic reticulum calcium ATPase (SERCA), the activity of which is impaired by obesity-induced changes in the PC/PE ratio of the ER (Fu et al., 2011) or by enrichment of the ER with saturated PC (Y. Li et al., 2004). Given the partial protection we saw using chemical chaperones, it is plausible that unfolded proteins could accumulate secondary to SFA-induced changes in ER membrane composition. However, any unfolded protein accumulation due to SFA treatment is likely mild, as it did not appear to engage the ATF6 α arm of the UPR in our studies.

The ability of UFAs to mitigate the lipotoxic effects of SFAs are well appreciated (L'homme et al., 2013; Montell et al., 2001; Welters et al., 2004), and UFAs have been proposed to do so by facilitating the incorporation of SFAs into TG and away from potentially deleterious metabolic pathways (Coll et al., 2008; Leamy et al., 2014; Listenberger et al., 2003). Consistent with this, we previously showed that increasing TG synthesis capacity in MCs by overexpressing DGAT1 was anti-inflammatory against SFAs *in vitro* or in the context of mice fed a HFD (Koliwad et al., 2010). Here, however, we found that OA co-treatment did not enhance PA flux

to TG, and that altering DGAT1 activity or expression did not affect SFA-induced IRE1 α or NLRP3 inflammasome activation.

Instead, we found that co-treatment with DOPC reproduces the protective effect of OA co-treatment, supporting the concept that the flux of OA itself into PC and/or other phospholipids counteracts the effect of SFA treatment on membrane saturation. Furthermore, DOPC also protected against IRE1 α activation stimulated by thapsigargin, suggesting that increased membrane fluidity may also limit the activation of IRE1 α in response to unfolded proteins. OA co-treatment does not have this effect, but it may not alter ER membrane fluidity to the same degree as direct supplementation with DOPC.

What are the physiological consequences of SFA-induced IRE1 α activation in MCs? We show a progressive rise in IRE1 α activity in tissues of mice consuming a diet rich in saturated fat, including the ATM compartment of WAT, and our findings imply that MCs exposed to SFAs undergo a sustained form of IRE1 α activation that fails to resolve, yet does not transition to a terminal program. As this unremitting form of IRE1 α activation is coupled with NLRP3 inflammasome activation both *in vitro* and in the ATMs of mice fed a HFD, our findings could help explain what promotes MCs in metabolic tissues to persistently propagate metabolic inflammation in the context of DIO. Additionally, our findings suggest that features of the chronic, low-level inflammation seen in DIO may be cell-autonomous, and targeting the intracellular pathways driving these programs could be effective in limiting metabolic inflammation and its consequences.

However, prior efforts to block inflammatory pathways in the context of DIO have been hampered by a lack of specificity that is problematic, as general immunosuppression can result in an unacceptable vulnerability to infection. Importantly, we show here that inhibiting IRE1 α , or

the membrane perturbations that lead to its activation, abolishes IL-1 β secretion stimulated by SFAs without affecting NLRP3 inflammasome activation in response to other triggers associated with infection or tissue damage. Though there are other implications of targeting this pathway that require further study, we have uncovered a mechanism for SFA-induced activation of IRE1 α and the NLRP3 inflammasome with translational implications relevant to combating metabolic inflammation without impairing acute inflammatory responses to pathogens.

REFERENCES

- Acosta-Alvear, D., Zhou, Y., Blais, A., Tsikitis, M., Lents, N.H., Arias, C., Lennon, C.J., Kluger, Y., Dynlacht, B.D., 2007. XBP1 controls diverse cell type- and condition-specific transcriptional regulatory networks. *Mol. Cell* 27, 53–66. doi:10.1016/j.molcel.2007.06.011
- Anderson, E.K., Hill, A.A., Hasty, A.H., 2012. Stearic Acid Accumulation in Macrophages Induces Toll-Like Receptor 4/2-Independent Inflammation Leading to Endoplasmic Reticulum Stress-Mediated Apoptosis. *Arteriosclerosis, Thrombosis, and Vascular Biology* 32, 1687–1695. doi:10.1161/ATVBAHA.112.250142
- Ariyama, H., Kono, N., Matsuda, S., Inoue, T., Arai, H., 2010. Decrease in membrane phospholipid unsaturation induces unfolded protein response. *Journal of Biological Chemistry* 285, 22027–22035. doi:10.1074/jbc.M110.126870
- Arkan, M.C., Hevener, A.L., Greten, F.R., Maeda, S., Li, Z.-W., Long, J.M., Wynshaw-Boris, A., Poli, G., Olefsky, J., Karin, M., 2005. IKK-beta links inflammation to obesity-induced insulin resistance. *Nature Medicine* 11, 191–198. doi:10.1038/nm1185
- Baccarella, A., Fontana, M.F., Chen, E.C., Kim, C.C., 2013. Toll-like receptor 7 mediates early innate immune responses to malaria. *Infect. Immun.* 81, 4431–4442. doi:10.1128/IAI.00923-13
- Beg, A.A., Finco, T.S., Nantermet, P.V., Baldwin, A.S., 1993. Tumor necrosis factor and interleukin-1 lead to phosphorylation and loss of I kappa B alpha: a mechanism for NF-kappa B activation. *Mol. Cell. Biol.* 13, 3301–3310.
- Bertolotti, A., Zhang, Y., Hendershot, L.M., Harding, H.P., Ron, D., 2000. Dynamic interaction of BiP and ER stress transducers in the unfolded-protein response. *Nat. Cell Biol.* 2, 326–332. doi:10.1038/35014014

- Bligh, E.G., Dyer, W.J., 1959. A rapid method of total lipid extraction and purification. *Can J Biochem Physiol* 37, 911–917.
- Borradaile, N.M., Han, X., Harp, J.D., Gale, S.E., Ory, D.S., Schaffer, J.E., 2006. Disruption of endoplasmic reticulum structure and integrity in lipotoxic cell death. *J. Lipid Res.* 47, 2726–2737. doi:10.1194/jlr.M600299-JLR200
- Boslem, E., MacIntosh, G., Preston, A.M., Bartley, C., Busch, A.K., Fuller, M., Laybutt, D.R., Meikle, P.J., Biden, T.J., 2011. A lipidomic screen of palmitate-treated MIN6 β -cells links sphingolipid metabolites with endoplasmic reticulum (ER) stress and impaired protein trafficking. *Biochem. J.* 435, 267–276. doi:10.1042/BJ20101867
- Brun, P., Castagliuolo, I., Di Leo, V., Buda, A., Pinzani, M., Palù, G., Martines, D., 2007. Increased intestinal permeability in obese mice: new evidence in the pathogenesis of nonalcoholic steatohepatitis. *Am. J. Physiol. Gastrointest. Liver Physiol.* 292, G518–25. doi:10.1152/ajpgi.00024.2006
- Cai, D., Yuan, M., Frantz, D.F., Melendez, P.A., Hansen, L., Lee, J., Shoelson, S.E., 2005. Local and systemic insulin resistance resulting from hepatic activation of IKK- β and NF- κ B. *Nature Medicine* 11, 183–190. doi:10.1038/nm1166
- Camell, C.D., Nguyen, K.Y., Jurczak, M.J., Shulman, G.I., Shadel, G.S., Dixit, V.D., 2015. Macrophage-specific de novo synthesis of ceramide is dispensable for inflammasome-driven inflammation and insulin-resistance in obesity. *J. Biol. Chem.* 290, 29402–29413.
- Cani, P.D., Amar, J., Iglesias, M.A., Poggi, M., Knauf, C., Bastelica, D., Neyrinck, A.M., Fava, F., Tuohy, K.M., Chabo, C., Waget, A., Delmée, E., Cousin, B., Sulpice, T., Chamontin, B., Ferrières, J., Tanti, J.-F., Gibson, G.R., Casteilla, L., Delzenne, N.M., Alessi, M.C., Burcelin, R., 2007. Metabolic endotoxemia initiates obesity and insulin resistance. *Diabetes*

56, 1761–1772. doi:10.2337/db06-1491

Cani, P.D., Bibiloni, R., Knauf, C., Waget, A., Neyrinck, A.M., Delzenne, N.M., Burcelin, R., 2008. Changes in gut microbiota control metabolic endotoxemia-induced inflammation in high-fat diet-induced obesity and diabetes in mice. *Diabetes* 57, 1470–1481.

doi:10.2337/db07-1403

Chen, H.C., Ladha, Z., Farese, R.V., 2002a. Deficiency of acyl coenzyme a:diacylglycerol acyltransferase 1 increases leptin sensitivity in murine obesity models. *Endocrinology* 143, 2893–2898. doi:10.1210/endo.143.8.8941

Chen, H.C., Stone, S.J., Zhou, P., Buhman, K.K., Farese, R.V., 2002b. Dissociation of obesity and impaired glucose disposal in mice overexpressing acyl coenzyme a:diacylglycerol acyltransferase 1 in white adipose tissue. *Diabetes* 51, 3189–3195.

Chopra, M., Galbraith, S., Darnton-Hill, I., 2002. A global response to a global problem: the epidemic of overnutrition. *Bull. World Health Organ.* 80, 952–958.

Coenen, K.R., Gruen, M.L., Lee-Young, R.S., Puglisi, M.J., Wasserman, D.H., Hasty, A.H., 2009. Impact of macrophage toll-like receptor 4 deficiency on macrophage infiltration into adipose tissue and the artery wall in mice. *Diabetologia* 52, 318–328. doi:10.1007/s00125-008-1221-7

Coll, T., Eyre, E., Rodríguez-Calvo, R., Palomer, X., Sánchez, R.M., Merlos, M., Laguna, J.C., Vázquez-Carrera, M., 2008. Oleate reverses palmitate-induced insulin resistance and inflammation in skeletal muscle cells. *J. Biol. Chem.* 283, 11107–11116.

doi:10.1074/jbc.M708700200

Credle, J.J., Finer-Moore, J.S., Papa, F.R., Stroud, R.M., Walter, P., 2005. On the mechanism of sensing unfolded protein in the endoplasmic reticulum. *Proc. Natl. Acad. Sci. U.S.A.* 102,

18773–18784. doi:10.1073/pnas.0509487102

Cunha, D.A., Hekerman, P., Ladrière, L., Bazarra-Castro, A., Ortis, F., Wakeham, M.C., Moore, F., Rasschaert, J., Cardozo, A.K., Bellomo, E., Overbergh, L., Mathieu, C., Lupi, R., Hai, T., Herchuelz, A., Marchetti, P., Rutter, G.A., Eizirik, D.L., Cnop, M., 2008. Initiation and execution of lipotoxic ER stress in pancreatic beta-cells. *J. Cell. Sci.* 121, 2308–2318. doi:10.1242/jcs.026062

de Roos, B., Rungapamestry, V., Ross, K., Rucklidge, G., Reid, M., Duncan, G., Horgan, G., Toomey, S., Browne, J., Loscher, C.E., Mills, K.H.G., Roche, H.M., 2009. Attenuation of inflammation and cellular stress-related pathways maintains insulin sensitivity in obese type I interleukin-1 receptor knockout mice on a high-fat diet. *Proteomics* 9, 3244–3256. doi:10.1002/pmic.200800761

Egnatchik, R.A., Leamy, A.K., Jacobson, D.A., Shiota, M., Young, J.D., 2014. ER calcium release promotes mitochondrial dysfunction and hepatic cell lipotoxicity in response to palmitate overload. *Mol Metab* 3, 544–553. doi:10.1016/j.molmet.2014.05.004

Erbay, E., Babaev, V.R., Mayers, J.R., Makowski, L., Charles, K.N., Snitow, M.E., Fazio, S., Wiest, M.M., Watkins, S.M., Linton, M.F., Hotamisligil, G.S., 2009. Reducing endoplasmic reticulum stress through a macrophage lipid chaperone alleviates atherosclerosis. *Nature Medicine* 15, 1383–1391. doi:10.1038/nm.2067

Erridge, C., Samani, N.J., 2009. Saturated fatty acids do not directly stimulate Toll-like receptor signaling. *Arteriosclerosis, Thrombosis, and Vascular Biology* 29, 1944–1949. doi:10.1161/ATVBAHA.109.194050

Fu, S., Yang, L., Li, P., Hofmann, O., Dicker, L., Hide, W., Lin, X., Watkins, S.M., Ivanov, A.R., Hotamisligil, G.S., 2011. Aberrant lipid metabolism disrupts calcium homeostasis

causing liver endoplasmic reticulum stress in obesity. *Nature* 473, 528–531.

doi:10.1038/nature09968

Galic, S., Fullerton, M.D., Schertzer, J.D., Sikkema, S., Marcinko, K., Walkley, C.R., Izon, D., Honeyman, J., Chen, Z.-P., van Denderen, B.J., Kemp, B.E., Steinberg, G.R., 2011.

Hematopoietic AMPK β 1 reduces mouse adipose tissue macrophage inflammation and insulin resistance in obesity. *J. Clin. Invest.* 121, 4903–4915. doi:10.1172/JCI58577DS1

Gollub, J., Sherlock, G., 2006. Clustering microarray data. *Meth. Enzymol.* 411, 194–213.

doi:10.1016/S0076-6879(06)11010-1

Han, D., Lerner, A.G., Vande Walle, L., Upton, J.-P., Xu, W., Hagen, A., Backes, B.J., Oakes, S.A., Papa, F.R., 2009. IRE1 α kinase activation modes control alternate

endoribonuclease outputs to determine divergent cell fates. *Cell* 138, 562–575.

doi:10.1016/j.cell.2009.07.017

Håversen, L., Danielsson, K.N., Fogelstrand, L., Wiklund, O., 2009. Induction of

proinflammatory cytokines by long-chain saturated fatty acids in human macrophages.

Atherosclerosis 202, 382–393. doi:10.1016/j.atherosclerosis.2008.05.033

Hirosumi, J., Tuncman, G., Chang, L., Görgün, C.Z., Uysal, K.T., Maeda, K., Karin, M.,

Hotamisligil, G.S., 2002. A central role for JNK in obesity and insulin resistance. *Nature*

420, 333–336. doi:10.1038/nature01137

Hollien, J., Lin, J.H., Li, H., Stevens, N., Walter, P., Weissman, J.S., 2009. Regulated Ire1-

dependent decay of messenger RNAs in mammalian cells. *J. Cell Biol.* 186, 323–331.

doi:10.1083/jcb.200903014

Holzer, R.G., Park, E.-J., Li, N., Tran, H., Chen, M., Choi, C., Solinas, G., Karin, M., 2011.

Saturated Fatty Acids Induce c-Src Clustering within Membrane Subdomains, Leading to

- JNK Activation. *Cell* 147, 173–184. doi:10.1016/j.cell.2011.08.034
- Huang, D.W., Sherman, B.T., Lempicki, R.A., 2009. Systematic and integrative analysis of large gene lists using DAVID bioinformatics resources. *Nat Protoc* 4, 44–57.
doi:10.1038/nprot.2008.211
- Iwawaki, T., Akai, R., Yamanaka, S., Kohno, K., 2009. Function of IRE1 alpha in the placenta is essential for placental development and embryonic viability. *Proc. Natl. Acad. Sci. U.S.A.* 106, 16657–16662. doi:10.1073/pnas.0903775106
- Jager, J., Grémeaux, T., Cormont, M., Le Marchand-Brustel, Y., Tanti, J.-F., 2007. Interleukin-1beta-induced insulin resistance in adipocytes through down-regulation of insulin receptor substrate-1 expression. *Endocrinology* 148, 241–251. doi:10.1210/en.2006-0692
- Kallio, K.A.E., Hätönen, K.A., Lehto, M., Salomaa, V., Männistö, S., Pussinen, P.J., 2015. Endotoxemia, nutrition, and cardiometabolic disorders. *Acta Diabetol* 52, 395–404.
doi:10.1007/s00592-014-0662-3
- Kaneko, M., Niinuma, Y., Nomura, Y., 2003. Activation signal of nuclear factor-kappa B in response to endoplasmic reticulum stress is transduced via IRE1 and tumor necrosis factor receptor-associated factor 2. *Biol. Pharm. Bull.* 26, 931–935.
- Kitai, Y., Ariyama, H., Kono, N., Oikawa, D., Iwawaki, T., Arai, H., 2013. Membrane lipid saturation activates IRE1 α without inducing clustering. *Genes Cells* 18, 798–809.
doi:10.1111/gtc.12074
- Knowler, W.C., Barrett-Connor, E., Fowler, S.E., Hamman, R.F., Lachin, J.M., Walker, E.A., Nathan, D.M., Diabetes Prevention Program Research Group, 2002. Reduction in the incidence of type 2 diabetes with lifestyle intervention or metformin. *N. Engl. J. Med.* 346, 393–403. doi:10.1056/NEJMoa012512

- Koliwad, S.K., Streeper, R.S., Monetti, M., Cornelissen, I., Chan, L., Terayama, K., Naylor, S., Rao, M., Hubbard, B., Farese, R.V., Jr., 2010. DGAT1-dependent triacylglycerol storage by macrophages protects mice from diet-induced insulin resistance and inflammation. *J. Clin. Invest.* 120, 756–767. doi:10.1172/JCI36066DS1
- Krahmer, N., Guo, Y., Wilfling, F., Hilger, M., Lingrell, S., Heger, K., Newman, H.W., Schmidt-Supprian, M., Vance, D.E., Mann, M., Farese, R.V., Walther, T.C., 2011. Phosphatidylcholine synthesis for lipid droplet expansion is mediated by localized activation of CTP:phosphocholine cytidyltransferase. *Cell Metabolism* 14, 504–515. doi:10.1016/j.cmet.2011.07.013
- Kratz, M., Coats, B.R., Hisert, K.B., Hagman, D., Mutskov, V., Peris, E., Schoenfelt, K.Q., Kuzma, J.N., Larson, I., Billing, P.S., Landerholm, R.W., Crouthamel, M., Gozal, D., Hwang, S., Singh, P.K., Becker, L., 2014. Metabolic Dysfunction Drives a Mechanistically Distinct Proinflammatory Phenotype in Adipose Tissue Macrophages. *Cell Metabolism* 20, 614–625. doi:10.1016/j.cmet.2014.08.010
- L'homme, L., Esser, N., Riva, L., Scheen, A., Paquot, N., Piette, J., Legrand-Poels, S., 2013. Unsaturated fatty acids prevent activation of NLRP3 inflammasome in human monocytes/macrophages. *J. Lipid Res.* 54, 2998–3008. doi:10.1194/jlr.M037861
- Leamy, A.K., Egnatchik, R.A., Shiota, M., Ivanova, P.T., Myers, D.S., Brown, H.A., Young, J.D., 2014. Enhanced synthesis of saturated phospholipids is associated with ER stress and lipotoxicity in palmitate treated hepatic cells. *J. Lipid Res.* 55. doi:10.1194/jlr.M050237
- Lee, A.-H., Iwakoshi, N.N., Glimcher, L.H., 2003. XBP-1 regulates a subset of endoplasmic reticulum resident chaperone genes in the unfolded protein response. *Mol. Cell. Biol.* 23, 7448–7459.

- Lee, J.Y., Sohn, K.H., Rhee, S.H., Hwang, D., 2001. Saturated fatty acids, but not unsaturated fatty acids, induce the expression of cyclooxygenase-2 mediated through Toll-like receptor 4. *J. Biol. Chem.* 276, 16683–16689. doi:10.1074/jbc.M011695200
- Lee, Y., Hirose, H., Ohneda, M., Johnson, J.H., McGarry, J.D., Unger, R.H., 1994. Beta-cell lipotoxicity in the pathogenesis of non-insulin-dependent diabetes mellitus of obese rats: impairment in adipocyte-beta-cell relationships. *Proc. Natl. Acad. Sci. U.S.A.* 91, 10878–10882.
- Lerner, A.G., Upton, J.-P., Praveen, P.V.K., Ghosh, R., Nakagawa, Y., Igarria, A., Shen, S., Nguyen, V., Backes, B.J., Heiman, M., Heintz, N., Greengard, P., Hui, S., Tang, Q., Trusina, A., Oakes, S.A., Papa, F.R., 2012. IRE1 α ; Induces Thioredoxin-Interacting Protein to Activate the NLRP3 Inflammasome and Promote Programmed Cell Death under Irremediable ER Stress. *Cell Metabolism* 16, 250–264. doi:10.1016/j.cmet.2012.07.007
- Li, H., Korennykh, A.V., Behrman, S.L., Walter, P., 2010. Mammalian endoplasmic reticulum stress sensor IRE1 signals by dynamic clustering. *Proc Natl Acad Sci USA* 107, 16113–16118. doi:10.1073/pnas.1010580107
- Li, Y., Ge, M., Ciani, L., Kuriakose, G., Westover, E.J., Dura, M., Covey, D.F., Freed, J.H., Maxfield, F.R., Lytton, J., Tabas, I., 2004. Enrichment of endoplasmic reticulum with cholesterol inhibits sarcoplasmic-endoplasmic reticulum calcium ATPase-2b activity in parallel with increased order of membrane lipids: implications for depletion of endoplasmic reticulum calcium stores and apoptosis in cholesterol-loaded macrophages. *J. Biol. Chem.* 279, 37030–37039. doi:10.1074/jbc.M405195200
- Listenberger, L.L., Han, X., Lewis, S.E., Cases, S., Farese, R.V., Ory, D.S., Schaffer, J.E., 2003. Triglyceride accumulation protects against fatty acid-induced lipotoxicity. *Proc. Natl. Acad.*

Sci. U.S.A. 100, 3077–3082. doi:10.1073/pnas.0630588100

Listenberger, L.L., Ory, D.S., Schaffer, J.E., 2001. Palmitate-induced Apoptosis Can Occur through a Ceramide-independent Pathway. *Journal of Biological Chemistry* 276, 14890–14895. doi:10.1074/jbc.M010286200

Look AHEAD Research Group, Wing, R.R., Bolin, P., Brancati, F.L., Bray, G.A., Clark, J.M., Coday, M., Crow, R.S., Curtis, J.M., Egan, C.M., Espeland, M.A., Evans, M., Foreyt, J.P., Ghazarian, S., Gregg, E.W., Harrison, B., Hazuda, H.P., Hill, J.O., Horton, E.S., Hubbard, V.S., Jakicic, J.M., Jeffery, R.W., Johnson, K.C., Kahn, S.E., Kitabchi, A.E., Knowler, W.C., Lewis, C.E., Maschak-Carey, B.J., Montez, M.G., Murillo, A., Nathan, D.M., Patricio, J., Peters, A., Pi-Sunyer, X., Pownall, H., Reboussin, D., Regensteiner, J.G., Rickman, A.D., Ryan, D.H., Safford, M., Wadden, T.A., Wagenknecht, L.E., West, D.S., Williamson, D.F., Yanovski, S.Z., 2013. Cardiovascular effects of intensive lifestyle intervention in type 2 diabetes. *N. Engl. J. Med.* 369, 145–154. doi:10.1056/NEJMoa1212914

Lumeng, C.N., Bodzin, J.L., Saltiel, A.R., 2007. Obesity induces a phenotypic switch in adipose tissue macrophage polarization. *J. Clin. Invest.* 117, 175–184. doi:10.1172/JCI29881

Maly, D.J., Papa, F.R., 2014. Druggable sensors of the unfolded protein response. *Nature Chemical Biology* 10, 892–901. doi:10.1038/nchembio.1664

Maris, M., Overbergh, L., Gysemans, C., Waget, A., Cardozo, A.K., Verdrengh, E., Cunha, J.P.M., Gotoh, T., Cnop, M., Eizirik, D.L., Burcelin, R., Mathieu, C., 2012. Deletion of C/EBP homologous protein (Chop) in C57Bl/6 mice dissociates obesity from insulin resistance. *Diabetologia* 55, 1167–1178. doi:10.1007/s00125-011-2427-7

Maurel, M., Chevet, E., Tavernier, J., Gerlo, S., 2014. Getting RIDD of RNA: IRE1 in cell fate regulation. *Trends Biochem. Sci.* 39, 245–254. doi:10.1016/j.tibs.2014.02.008

- Mekahli, D., Bultynck, G., Parys, J.B., De Smedt, H., Missiaen, L., 2011. Endoplasmic-Reticulum Calcium Depletion and Disease. *Cold Spring Harbor Perspectives in Biology* 3, a004317–a004317. doi:10.1101/cshperspect.a004317
- Montell, E., Turini, M., Marotta, M., Roberts, M., Noé, V., Ciudad, C.J., Macé, K., Gómez-Foix, A.M., 2001. DAG accumulation from saturated fatty acids desensitizes insulin stimulation of glucose uptake in muscle cells. *Am. J. Physiol. Endocrinol. Metab.* 280, E229–37.
- Nguyen, M.T.A., Favellyukis, S., Nguyen, A.-K., Reichart, D., Scott, P.A., Jenn, A., Liu-Bryan, R., Glass, C.K., Neels, J.G., Olefsky, J.M., 2007. A subpopulation of macrophages infiltrates hypertrophic adipose tissue and is activated by free fatty acids via Toll-like receptors 2 and 4 and JNK-dependent pathways. *J. Biol. Chem.* 282, 35279–35292. doi:10.1074/jbc.M706762200
- Orr, J.S., Puglisi, M.J., Ellacott, K.L.J., Lumeng, C.N., Wasserman, D.H., Hasty, A.H., 2012. Toll-like Receptor 4 Deficiency Promotes the Alternative Activation of Adipose Tissue Macrophages. *Diabetes*. doi:10.2337/db11-1595
- Osborn, O., Brownell, S.E., Sanchez-Alavez, M., Salomon, D., Gram, H., Bartfai, T., 2008. Treatment with an Interleukin 1 beta antibody improves glycemic control in diet-induced obesity. *Cytokine* 44, 141–148. doi:10.1016/j.cyto.2008.07.004
- Osowski, C.M., Hara, T., O'Sullivan-Murphy, B., Kanekura, K., Lu, S., Hara, M., Ishigaki, S., Zhu, L.J., Hayashi, E., Hui, S.T., Greiner, D., Kaufman, R.J., Bortell, R., Urano, F., 2012. Thioredoxin-Interacting Protein Mediates ER Stress-Induced Beta Cell Death through Initiation of the Inflammasome. *Cell Metabolism* 16, 265–273. doi:10.1016/j.cmet.2012.07.005
- Ostrander, D.B., Sparagna, G.C., Amoscato, A.A., McMillin, J.B., Dowhan, W., 2001.

- Decreased cardiolipin synthesis corresponds with cytochrome c release in palmitate-induced cardiomyocyte apoptosis. *J. Biol. Chem.* 276, 38061–38067. doi:10.1074/jbc.M107067200
- Ozcan, U., Cao, Q., Yilmaz, E., Lee, A.-H., Iwakoshi, N.N., Ozdelen, E., Tuncman, G., Görgün, C., Glimcher, L.H., Hotamisligil, G.S., 2004. Endoplasmic reticulum stress links obesity, insulin action, and type 2 diabetes. *Science* 306, 457–461. doi:10.1126/science.1103160
- Ozcan, U., Yilmaz, E., Ozcan, L., Furuhashi, M., Vaillancourt, E., Smith, R.O., Görgün, C.Z., Hotamisligil, G.S., 2006. Chemical chaperones reduce ER stress and restore glucose homeostasis in a mouse model of type 2 diabetes. *Science* 313, 1137–1140. doi:10.1126/science.1128294
- Pal, D., Dasgupta, S., Kundu, R., Maitra, S., Das, G., Mukhopadhyay, S., Ray, S., Majumdar, S.S., Bhattacharya, S., 2012. Fetuin-A acts as an endogenous ligand of TLR4 to promote lipid-induced insulin resistance. *Nature Medicine* 18, 1279–1285. doi:10.1038/nm.2851
- Park, B.S., Song, D.H., Kim, H.M., Choi, B.-S., Lee, H., Lee, J.-O., 2009. The structural basis of lipopolysaccharide recognition by the TLR4-MD-2 complex. *Nature* 458, 1191–1195. doi:10.1038/nature07830
- Patsouris, D., Li, P.-P., Thapar, D., Chapman, J., Olefsky, J.M., Neels, J.G., 2008. Ablation of CD11c-Positive Cells Normalizes Insulin Sensitivity in Obese Insulin Resistant Animals. *Cell Metabolism* 8, 301–309. doi:10.1016/j.cmet.2008.08.015
- Poltorak, A., He, X., Smirnova, I., Liu, M.Y., Van Huffel, C., Du, X., Birdwell, D., Alejos, E., Silva, M., Galanos, C., Freudenberg, M., Ricciardi-Castagnoli, P., Layton, B., Beutler, B., 1998. Defective LPS signaling in C3H/HeJ and C57BL/10ScCr mice: mutations in *Tlr4* gene. *Science* 282, 2085–2088.
- Promlek, T., Ishiwata-Kimata, Y., Shido, M., Sakuramoto, M., Kohno, K., Kimata, Y., 2011.

- Membrane aberrancy and unfolded proteins activate the endoplasmic reticulum stress sensor Ire1 in different ways. *Mol. Biol. Cell* 22, 3520–3532. doi:10.1091/mbc.E11-04-0295
- Qi, L., Yang, L., Chen, H., 2011. Detecting and quantitating physiological endoplasmic reticulum stress. *Meth. Enzymol.* 490, 137–146. doi:10.1016/B978-0-12-385114-7.00008-8
- Reynolds, C.M., McGillicuddy, F.C., Harford, K.A., Finucane, O.M., Mills, K.H.G., Roche, H.M., 2012. Dietary saturated fatty acids prime the NLRP3 inflammasome via TLR4 in dendritic cells-implications for diet-induced insulin resistance. *Mol. Nutr. Food Res.* 56, 1212–1222. doi:10.1002/mnfr.201200058
- Saberi, M., Woods, N.-B., de Luca, C., Schenk, S., Lu, J.C., Bandyopadhyay, G., Verma, I.M., Olefsky, J.M., 2009. Hematopoietic cell-specific deletion of toll-like receptor 4 ameliorates hepatic and adipose tissue insulin resistance in high-fat-fed mice. *Cell Metabolism* 10, 419–429. doi:10.1016/j.cmet.2009.09.006
- Saldanha, A.J., 2004. Java Treeview--extensible visualization of microarray data. *Bioinformatics* 20, 3246–3248. doi:10.1093/bioinformatics/bth349
- Schaeffler, A., Gross, P., Buettner, R., Bollheimer, C., Buechler, C., Neumeier, M., Kopp, A., Schoelmerich, J., Falk, W., 2009. Fatty acid-induced induction of Toll-like receptor-4/nuclear factor- κ B pathway in adipocytes links nutritional signalling with innate immunity. *Immunology* 126, 233–245. doi:10.1111/j.1365-2567.2008.02892.x
- Schilling, J.D., Machkovech, H.M., He, L., Sidhu, R., Fujiwara, H., Weber, K., Ory, D.S., Schaffer, J.E., 2012. Palmitate and LPS trigger synergistic ceramide production in primary macrophages. *Journal of Biological Chemistry* 288, 2923–2932. doi:10.1074/jbc.M112.419978
- Sharma, N.K., Das, S.K., Mondal, A.K., Hackney, O.G., Chu, W.S., Kern, P.A., Rasouli, N.,

- Spencer, H.J., Yao-Borengasser, A., Elbein, S.C., 2008. Endoplasmic reticulum stress markers are associated with obesity in nondiabetic subjects. *J. Clin. Endocrinol. Metab.* 93, 4532–4541. doi:10.1210/jc.2008-1001
- Shi, H., Kokoeva, M.V., Inouye, K., Tzameli, I., Yin, H., Flier, J.S., 2006. TLR4 links innate immunity and fatty acid–induced insulin resistance. *J. Clin. Invest.* 116, 3015–3025. doi:10.1172/JCI28898
- So, J.-S., Hur, K.Y., Tarrío, M., Ruda, V., Frank-Kamenetsky, M., Fitzgerald, K., Kotliansky, V., Lichtman, A.H., Iwawaki, T., Glimcher, L.H., Lee, A.-H., 2012. Silencing of lipid metabolism genes through IRE1 α -mediated mRNA decay lowers plasma lipids in mice. *Cell Metabolism* 16, 487–499. doi:10.1016/j.cmet.2012.09.004
- Solinas, G., Vilcu, C., Neels, J.G., Bandyopadhyay, G.K., Luo, J.-L., Naugler, W., Grivennikov, S., Wynshaw-Boris, A., Scadeng, M., Olefsky, J.M., Karin, M., 2007. JNK1 in Hematopoietically Derived Cells Contributes to Diet-Induced Inflammation and Insulin Resistance without Affecting Obesity. *Cell Metabolism* 6, 386–397. doi:10.1016/j.cmet.2007.09.011
- Stefanovic-Racic, M., Yang, X., Turner, M.S., Mantell, B.S., Stolz, D.B., Sumpter, T.L., Sipula, I.J., Dedousis, N., Scott, D.K., Morel, P.A., Thomson, A.W., O'Doherty, R.M., 2012. Dendritic Cells Promote Macrophage Infiltration and Comprise a Substantial Proportion of Obesity-Associated Increases in CD11c⁺ Cells in Adipose Tissue and Liver. *Diabetes*. doi:10.2337/db11-1523
- Stienstra, R., Joosten, L.A.B., Koenen, T., van Tits, B., van Diepen, J.A., van den Berg, S.A.A., Rensen, P.C.N., Voshol, P.J., Fantuzzi, G., Hijmans, A., Kersten, S., Müller, M., van den Berg, W.B., van Rooijen, N., Wabitsch, M., Kullberg, B.-J., van der Meer, J.W.M.,

- Kanneganti, T., Tack, C.J., Netea, M.G., 2010. The inflammasome-mediated caspase-1 activation controls adipocyte differentiation and insulin sensitivity. *Cell Metabolism* 12, 593–605. doi:10.1016/j.cmet.2010.11.011
- Suganami, T., Tanimoto-Koyama, K., Nishida, J., Itoh, M., Yuan, X., Mizuarai, S., Kotani, H., Yamaoka, S., Miyake, K., Aoe, S., Kamei, Y., Ogawa, Y., 2007. Role of the Toll-like Receptor 4/NF- κ B Pathway in Saturated Fatty Acid-Induced Inflammatory Changes in the Interaction Between Adipocytes and Macrophages. *Arteriosclerosis, Thrombosis, and Vascular Biology* 27, 84–91. doi:10.1161/01.ATV.0000251608.09329.9a
- Tomlinson, M.G., Kane, L.P., Su, J., Kadlecsek, T.A., Mollenauer, M.N., Weiss, A., 2004. Expression and function of Tec, Itk, and Btk in lymphocytes: evidence for a unique role for Tec. *Mol. Cell. Biol.* 24, 2455–2466.
- Tsukano, H., Gotoh, T., Endo, M., Miyata, K., Tazume, H., Kadomatsu, T., Yano, M., Iwawaki, T., Kohno, K., Araki, K., Mizuta, H., Oike, Y., 2010. The endoplasmic reticulum stress-C/EBP homologous protein pathway-mediated apoptosis in macrophages contributes to the instability of atherosclerotic plaques. *Arteriosclerosis, Thrombosis, and Vascular Biology* 30, 1925–1932. doi:10.1161/ATVBAHA.110.206094
- Turnbaugh, P.J., Ley, R.E., Mahowald, M.A., Magrini, V., Mardis, E.R., Gordon, J.I., 2006. An obesity-associated gut microbiome with increased capacity for energy harvest. *Nature* 444, 1027–131. doi:10.1038/nature05414
- Tusher, V.G., Tibshirani, R., Chu, G., 2001. Significance analysis of microarrays applied to the ionizing radiation response. *Proc. Natl. Acad. Sci. U.S.A.* 98, 5116–5121. doi:10.1073/pnas.091062498
- Urano, F., Wang, X., Bertolotti, A., Zhang, Y., Chung, P., Harding, H.P., Ron, D., 2000.

- Coupling of stress in the ER to activation of JNK protein kinases by transmembrane protein kinase IRE1. *Science* 287, 664–666.
- Vandanmagsar, B., Youm, Y.-H., Ravussin, A., Galgani, J.E., Stadler, K., Mynatt, R.L., Ravussin, E., Stephens, J.M., Dixit, V.D., 2011. The NLRP3 inflammasome instigates obesity-induced inflammation and insulin resistance. *Nature Medicine* 17, 179–188.
doi:10.1038/nm.2279
- Vitiello, F., Zanetta, J.P., 1978. Thin-layer chromatography of phospholipids. *J. Chromatogr.* 166, 637–640.
- Volmer, R., Ron, D., 2015. Lipid-dependent regulation of the unfolded protein response. *Curr. Opin. Cell Biol.* 33, 67–73. doi:10.1016/j.ceb.2014.12.002
- Volmer, R., van der Ploeg, K., Ron, D., 2013. Membrane lipid saturation activates endoplasmic reticulum unfolded protein response transducers through their transmembrane domains. *Proc Natl Acad Sci USA* 110, 4628–4633. doi:10.1073/pnas.1217611110
- Wadden, T.A., Webb, V.L., Moran, C.H., Bailer, B.A., 2012. Lifestyle modification for obesity: new developments in diet, physical activity, and behavior therapy. *Circulation* 125, 1157–1170. doi:10.1161/CIRCULATIONAHA.111.039453
- Wang, D., Wei, Y., Pagliassotti, M.J., 2006. Saturated fatty acids promote endoplasmic reticulum stress and liver injury in rats with hepatic steatosis. *Endocrinology* 147, 943–951. doi:10.1210/en.2005-0570
- Wang, L., Perera, B.G.K., Hari, S.B., Bhatarai, B., Backes, B.J., Seeliger, M.A., Schürer, S.C., Oakes, S.A., Papa, F.R., Maly, D.J., 2012. Divergent allosteric control of the IRE1 α endoribonuclease using kinase inhibitors. *Nature Chemical Biology* 8, 982–989.
doi:10.1038/nchembio.1094

- Wei, Y., Wang, D., Gentile, C.L., Pagliassotti, M.J., 2009. Reduced endoplasmic reticulum luminal calcium links saturated fatty acid-mediated endoplasmic reticulum stress and cell death in liver cells. *Mol Cell Biochem* 331, 31–40. doi:10.1007/s11010-009-0142-1
- Weisberg, S.P., McCann, D., Desai, M., Rosenbaum, M., Leibel, R.L., Ferrante, A.W., 2003. Obesity is associated with macrophage accumulation in adipose tissue. *J. Clin. Invest.* 112, 1796–1808. doi:10.1172/JCI19246
- Welters, H.J., Tadayyon, M., Scarpello, J.H.B., Smith, S.A., Morgan, N.G., 2004. Mono-unsaturated fatty acids protect against beta-cell apoptosis induced by saturated fatty acids, serum withdrawal or cytokine exposure. *FEBS Lett.* 560, 103–108. doi:10.1016/S0014-5793(04)00079-1
- Wen, H., Gris, D., Lei, Y., Jha, S., Zhang, L., Huang, M.T.-H., Brickey, W.J., Ting, J.P.-Y., 2011. Fatty acid-induced NLRP3-ASC inflammasome activation interferes with insulin signaling. *Nat Immunol* 12, 408–415. doi:10.1038/ni.2022
- World Health Organization, 1997. The World Health Report 1997--conquering suffering, enriching humanity. *World Health Forum* 18, 248–260.
- Xu, X., Grijalva, A., Skowronski, A., van Eijk, M., Serlie, M.J., Ferrante, A.W., 2013. Obesity activates a program of lysosomal-dependent lipid metabolism in adipose tissue macrophages independently of classic activation. *Cell Metabolism* 18, 816–830. doi:10.1016/j.cmet.2013.11.001
- Xue, J., Schmidt, S.V., Sander, J., Draffehn, A., Krebs, W., Quester, I., De Nardo, D., Gohel, T.D., Emde, M., Schmidleithner, L., Ganesan, H., Nino-Castro, A., Mallmann, M.R., Labzin, L., Theis, H., Kraut, M., Beyer, M., Latz, E., Freeman, T.C., Ulas, T., Schultze, J.L., 2014. Transcriptome-based network analysis reveals a spectrum model of human macrophage

activation. *Immunity* 40, 274–288. doi:10.1016/j.immuni.2014.01.006

Yuan, M., Konstantopoulos, N., Lee, J., Hansen, L., Li, Z.W., Karin, M., Shoelson, S.E., 2001.

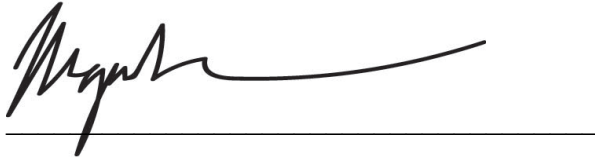
Reversal of obesity- and diet-induced insulin resistance with salicylates or targeted

disruption of *Ikkbeta*. *Science* 293, 1673–1677. doi:10.1126/science.1061620

PUBLISHING AGREEMENT

It is the policy of the University to encourage the distribution of all theses, dissertations, and manuscripts. Copies of all UCSF theses, dissertations, and manuscripts will be routed to the library via the Graduate Division. The library will make all theses, dissertations, and manuscripts accessible to the public and will preserve these to the best of their abilities, in perpetuity.

I hereby grant permission to the Graduate Division of the University of California, San Francisco to release copies of my thesis, dissertation, or manuscript to the Campus Library to provide access and preservation, in whole or in part, in perpetuity.

A handwritten signature in black ink, appearing to be 'Megan', written over a horizontal line.

Author Signature

8/31/2016

Date